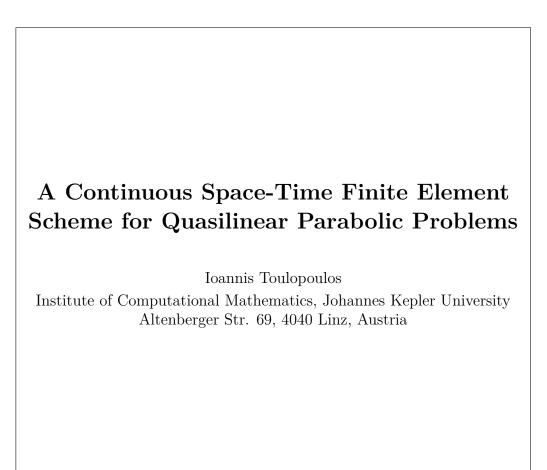


JOHANNES KEPLER UNIVERSITY LINZ



Institute of Computational Mathematics



NuMa-Report No. 2021-01

February 2021

A–4040 LINZ, Altenbergerstraße 69, Austria

Technical Reports before 1998:

1995

95-1	Hedwig Brandstetter	
05.9	Was ist neu in Fortran 90?	March 1995
95-2	G. Haase, B. Heise, M. Kuhn, U. Langer Adaptive Domain Decomposition Methods for Finite and Boundary Element Equations.	August 1995
95-3	Joachim Schöberl	
	An Automatic Mesh Generator Using Geometric Rules for Two and Three Space Dimensions.	August 1995
1996		
96-1	Ferdinand Kickinger	
	Automatic Mesh Generation for 3D Objects.	February 1996
96-2	Mario Goppold, Gundolf Haase, Bodo Heise und Michael Kuhn	
	Preprocessing in BE/FE Domain Decomposition Methods.	February 1996
96-3	Bodo Heise	
	A Mixed Variational Formulation for 3D Magnetostatics and its Finite Element	February 1996
06.4	Discretisation.	
96-4	Bodo Heise und Michael Jung Robust Parallel Newton-Multilevel Methods.	February 1996
96-5	Ferdinand Kickinger	rebruary 1990
00 0	Algebraic Multigrid for Discrete Elliptic Second Order Problems.	February 1996
96-6	Bodo Heise	v
	A Mixed Variational Formulation for 3D Magnetostatics and its Finite Element Discretisation.	May 1996
96-7	Michael Kuhn	
	Benchmarking for Boundary Element Methods.	June 1996
1997		
97-1	Bodo Heise, Michael Kuhn and Ulrich Langer	
	A Mixed Variational Formulation for 3D Magnetostatics in the Space $H(rot) \cap H(div)$	February 1997
97-2	Joachim Schöberl	
	Robust Multigrid Preconditioning for Parameter Dependent Problems I: The Stokes-type Case.	June 1997
97-3	Ferdinand Kickinger, Sergei V. Nepomnyaschikh, Ralf Pfau, Joachim Schöberl	
	Numerical Estimates of Inequalities in $H^{\frac{1}{2}}$.	August 1997
97-4	Joachim Schöberl	

Programmbeschreibung NAOMI 2D und Algebraic Multigrid. September 1997

From 1998 to 2008 technical reports were published by SFB013. Please see

http://www.sfb013.uni-linz.ac.at/index.php?id=reports From 2004 on reports were also published by RICAM. Please see

http://www.ricam.oeaw.ac.at/publications/list/ For a complete list of NuMa reports see

http://www.numa.uni-linz.ac.at/Publications/List/

A continuous space-time finite element scheme for quasilinear parabolic problems

I. Toulopoulos¹

¹ Institute of Computational Mathematics, Johannes Kepler University Altenberger Strasse 69 A-4040 Linz Austria ioannis.toulopoulos@jku.at

Abstract

In this paper continuous space-time finite element (FE) methods are developed for approximating a class of quasilinear parabolic problems in space and in time simultaneously. The whole approach is based on a space-time variational formulation where streamline upwind terms are further added for stabilizing the discretization in time direction. Error estimates are shown and are verified numerically through a series of numerical tests. Emphasis is placed on investigating the asymptotic convergence of the error parts which are related to the time discretization.

Keywords: quasilinear parabolic equations, parabolic *p*-Laplacian, continuous space-time finite element discretizations, a-priori error estimates, asymptotic convergence rates

1 Introduction

The description of real-life phenomena very often leads to second order parabolic problems of the form $u_t - Lu = f$, where L is a second order differential operator, [13], with most common the case where $L := -\Delta$. The numerical solution of these problems has been a subject of investigation of many authors in the past decades. The usual discretization procedures are first apply a Galerkin discretization in space, to reduce the problem to a system of ordinary differential equations. Then an appropriate method, e.g., a Runge-Kutta, is applied for integrating this last system in time. Also fully discretization schemes can be derived by applying Galerkin techniques in both space and time, [32], which can be usually reformulated in a version of a quadrature rule for integration in time. The final space-time mesh of these approaches is a tensor product structured mesh (i.e., each mesh element is a tensor product between the spatial element and the time interval) with some restriction between the size of the time step and the size of the space mesh. The above methods use some kind of time-stepping techniques for time discretization, which in general can cause further difficulties when extra refined meshes are used for resolving interesting features of the solution.

Last years space-time FE methods have been proposed for solving time evolution or parabolic problems, [20]. These methods based on a unified space-time variational formulation and are free from the restrictions between the space and time mesh size. The main idea is to see the time variable t as another variable, lets say, x_{d_x+1} , in the direction d_x+1 , if $x_1, ..., x_{d_x}$, are the spatial variables. In that way the time derivative u_t plays the role of a strong convection in the direction x_{d_x+1} . This consideration makes a unified FE discretization in time and in space feasible.

The use of FE in space and in time for parabolic problems is not new. In the past a number of different forms of space-time FE methods have been investigated and applied to several problems, see, e.g., [3, 4], [18], [16], [30], see also the survey paper [31] for applications to engineering problems. Last years stabilized spacetime FE approaches have been extensively analysed and proposed for solving linear parabolic problems. In [24], [2], [29] stability properties of space-time methods have been investigated in the frame of Petrov-Galrkin discretizations using different trial and test spaces which satisfy a discrete inf-sup condition. In [28], tensor product wavelet bases have been constructed for reformulating the parabolic problem as a well-posed bi-infinite matrix vector problem which if finally discretized by an adaptive method, see also [8]. Working in different direction subgrid viscosity stabilization techniques using bubble functions have been investigating in [33]. In general, for developing the space-time FE schemes, similar to the current work, we usually first set up an appropriate weak space-time variational formulation. We multiply the parabolic problem with a test function depending on space and on time and then integrate with respect on both space and time, [9], [37], see also discussion in [22] for linear problems. As it is mentioned above in the present space-time formulation the time derivative plays the role of an advection term. For this reason upwind streamline diffusion techniques, (cf. [15]), have been utilized for achieving stability, see, e.g., [27] for linear problems with low regularity, and [23] for an extension to Isogeometric Analysis framework.

In contrast to the linear problems, there are no many works for nonlinear parabolic problems. We indicatively mention the works [12] and [35], where discontinuous in time and continuous in space FE methods have been analysed for nonlinear problems. In general the parabolic *p*-Laplacian problems may have solutions with different regularity properties in space and in time, [9]. In [5] appropriate regularity assumptions for the solution u have been introduced for proving optimal convergence rates for continuous FE approximations in space and backward Euler in time. Optimal convergence rates for the same discretizations have been shown in [10] but under more general considerations of the problem. In [19] numerical solutions have been presented for the similar problems using discontinuous Galerkin in space and high order Runge-Kutta methods in time.

In this work a stable space-time FE method is presented and analyzed to discretize in space and in time simultaneously scalar quasilinear parabolic problems of the form $u_t - \operatorname{div} \mathbf{A}(\nabla_x u) = f$, where $u_t := \partial_t u$, $\nabla_x u$ is the spatial gradient of u and $\mathbf{A}(\nabla_x u) = (\varepsilon + |\nabla_x u|)^{p-2} \nabla_x u$, with the parameters $\varepsilon > 0$ and 1 < p. In general they can be seen as variations of the parabolic p-Laplacian problem where $\varepsilon = 0$. Here we mainly consider the case of $\varepsilon = 1$ and 1 . Our work is the first study of continuous space-time FE methods applied to the previous quasilinear problems. The whole numerical approach is based on a weak space-time formulation. Following the main ideas used in the linear problems, we introduce upwind streamline diffusion terms for stabilizing the time discretization. We estimate the error in an appropriate mesh dependent norm denoted by $\|\cdot\|_h$, see (3.29). The error terms related to the time discretization are multiplied with a stability parameter $\tau := \tau(h)$ defined through the error analysis. On the other hand the error related to the space discretization is estimated by means of quasi-norms introduced in [11]. In the error analysis a global regularity $u \in W^{2,p}$ in the space-time cylinder is assumed which enable us to apply usual interpolation estimates and consequently to derive uniform error estimates in space and in time. Typically one can expect different regularity properties for the solution u of the evolutionary problem, i.e., $u_t \in L^2$ and $\partial_{x_i} u \in W^{1,p}$, $i = 1, \ldots, d_x$, [9]. Anyway the previous regularity assumption does not prevent this case. In the numerical examples we investigate the asymptotic convergence behavior of the error when the solution exhibits different regularity properties in space and in time. This is the first time that space-time FE methods are applied for solving quasilinear parabolic *p*-Laplace type problems. The outcome of this work is that space-time FE methodologies accompanied with stream-line diffusion stability terms can have good stability properties and high accuracy (with respect to the solution regularity). Moreover, as we show in the numerical tests, anisotropic mesh refinement can be applied for recovering optimal convergence properties with respect to the polynomial space. All the previous features can be combined with fast space-time parallel solvers, see e.g., [17], for implementations in Isogeometric Analysis. In addition they can be combined with adaptive techniques without the time mesh size to be necessarily small, which offers great flexibility during the solution of realistic problems. Finally, we note that the analysis of the case, where the solution will exhibit an anisotropic regularity behavior between the time and space direction, is the subject of a forthcoming work.

An outline of the paper is as follows. In Section 2 some preliminaries together with the notation of the related Sobolev spaces are given. In Section 3 the parabolic problem is given and the weak-space time formulation is described. In the last part of Section 3 the FE discretization in presented and the discretization error analysis is developed. Finally, in Section 4 we show a series of numerical examples for verifying the theoretical results. The paper closes with the conclusions.

2 Preliminaries

2.1 Notations

Let Ω be a bounded Lipschitz domain in \mathbb{R}^d , d = 1, ..., 4, with boundary $\Gamma = \partial \Omega$. For any multi-index $\boldsymbol{\alpha}_d = (\alpha_1, \ldots, \alpha_d)$ of non-negative integers $\alpha_1, \ldots, \alpha_d$, we define the differential operator $\partial_x^{\boldsymbol{\alpha}_d} = \partial_{x_1}^{\alpha_1} \ldots \partial_{x_d}^{\alpha_d}$, with $\partial_{x_j} = \partial/\partial x_j$, $j = 1, \ldots, d$. Let $1 \leq p \leq \infty$ be fixed and ℓ be a non-negative integer. As usual, $L^p(\Omega)$ denotes the Lebesgue spaces for which $\int_{\Omega} |\phi(x)|^p dx < \infty$, endowed with the norm $\|\phi\|_{L^p(\Omega)} =$ $\left(\int_{\Omega} |\phi(x)|^p dx\right)^{\frac{1}{p}}$, and $W^{\ell,p}(\Omega)$ is the Sobolev space, which consists of the functions $\phi: \Omega \to \mathbb{R}$ such that their weak derivatives $\partial_x^{\boldsymbol{\alpha}_d} \phi$ with $|\boldsymbol{\alpha}_d| \leq \ell$ exist and belong to $L^p(\Omega)$. If $\phi \in W^{\ell,p}(\Omega)$, then its norm is defined by

$$\|\phi\|_{W^{\ell,p}(\Omega)} = \Big(\sum_{0 \le |\alpha| \le \ell} \|\partial_x^{\alpha_d} \phi\|_{L^p(\Omega)}^p\Big)^{\frac{1}{p}} \quad \text{and} \quad \|\phi\|_{W^{\ell,\infty}(\Omega)} = \max_{0 \le |\alpha| \le \ell} \|\partial_x^{\alpha_d} \phi\|_{\infty},$$

for $1 \le p < \infty$ and $p = \infty$, respectively. We further define the spaces

$$W_0^{\ell,p}(\Omega) := \{ \phi \in W^{\ell,p}(\Omega) \text{ such that } \phi|_{\partial\Omega} = 0 \},$$
(2.1a)

$$W^{\ell,p}_{\Gamma}(\Omega) := \{ \phi \in W^{\ell,p}(\Omega) \text{ such that } \phi|_{\Gamma \subset \partial\Omega} = 0 \}.$$
(2.1b)

We refer the reader to [1] for more details about Sobolev spaces

2.2 Spaces on the space-time domain

Let J = (0,T) be the time interval with some final time T > 0 and let Ω be a bounded domain in \mathbb{R}^{d_x} , $d_x = 1, 2$ or 3. For later use, we consider the space-time cylinder $Q \subset \mathbb{R}^d$ with $d = d_x + 1$, defined by $Q = \Omega \times J$, and its boundary parts $\Sigma = \partial \Omega \times J$, $\Sigma_T = \Omega \times \{T\}$ and $\Sigma_0 = \Omega \times \{0\}$ such that $\partial Q = \Sigma \cup \overline{\Sigma}_0 \cup \overline{\Sigma}_T$. Accordingly to the definition of $\partial_x^{\alpha_d}$, we now define the operator $\partial_x^{\alpha_{d_x}}$ and also define the spatial gradient $\nabla_x \phi = (\partial_{x_1} \phi, \dots, \partial_{x_{d_x}} \phi)$, and the whole gradient $\nabla \phi := (\partial_t \phi, \nabla_x \phi)$. Let the vector $\boldsymbol{\ell} = (\ell_t, \ell_x)$ with ℓ_t and ℓ_x to be positive integers, and let the vector $\mathbf{p} = (p_t, p_x)$ with entries $p_t > 1$ and $p_x > 1$. We consider the class of functions defined on the space-time cylinder Q, with weak derivatives $\partial_x^{|\alpha_{d_x}| \leq \ell_x} \phi \in L^{p_x}(Q)$ and $\partial_t^{i \leq \ell_t} \phi \in L^{p_t}(Q)$, i.e.,

$$W^{\ell,p}(Q) = \{ \phi \in L_{p_x}(Q) : \partial_x^{\boldsymbol{\alpha}_{d_x}} \phi \in L_{p_x}(Q) \text{ for } 0 \le |\boldsymbol{\alpha}_{d_x}| \le \ell_x, \text{ and} \\ \phi \in L_{p_t}(Q) : \partial_t^i \phi \in L_{p_t}(Q), \ i = 1, ..., \ell_t \}.$$

$$(2.2)$$

If $\ell_x = \ell_t = \ell$, instead of $W^{\ell,\mathbf{p}}$ we simply write $W^{\ell,\mathbf{p}}$. In the analysis below, we particularly use the space where $\ell_t = \ell_x = 1$, $p_t = 2$ and $p_x = p$, i.e., $\phi \in W^{1,\mathbf{p}=(2,p)}(Q)$, with associated norm

$$\|\phi\|_{W^{1,\mathbf{p}}(Q)} = \|\phi\|_{L_2(Q)} + \|\partial_t \phi\|_{L_2(Q)} + \sum_{|\boldsymbol{\alpha}_{d_x}|=1} \|\partial_x^{\boldsymbol{\alpha}_{d_x}}\phi\|_{L^p(Q)}.$$
(2.3)

Note that for $1 , if <math>\phi \in L^2(Q)$ then $\phi \in L^p(Q)$. Let $\ell = (0, 1)$ and $\mathbf{p} = (2, p)$. In view of (2.1) and (2.2) we introduce the subspaces

$$W_0^{\ell,\mathbf{p}}(Q) = \{ \phi \in L_2(Q) : \nabla_x \phi \in [L_p(Q)]^d, \ \phi = 0 \text{ on } \Sigma \},$$
(2.4a)

$$W_{0,\bar{0}}^{1,\mathbf{p}}(Q) = \{ \phi \in L_2(Q) : \nabla_x \phi \in [L_p(Q)]^d, \, \partial_t \phi \in L_2(Q), \, \phi = 0 \text{ on } \Sigma \cup \Sigma_T \}, \quad (2.4b)$$

$$W_{0,\underline{0}}^{1,\mathbf{p}}(Q) = \{\phi \in L_2(Q) : \nabla_x \phi \in [L_p(Q)]^d, \, \partial_t \phi \in L_2(Q), \phi = 0 \text{ on } \Sigma \cup \Sigma_0\}.$$
(2.4c)

2.3 Known inequalities

The following inequalities are going to be used in several places in the text. Hölder's and Young's inequalities read: For any δ , $0 < \delta < \infty$, and $1 \le p, q \le \infty$ such that $\frac{1}{p} + \frac{1}{q} = 1$, for $f \in L^p(Q)$ and $g \in L^q(Q)$, there holds

$$\left| \int_{Q} fg \, dx \right| \le \|f\|_{L^{p}(Q)} \|g\|_{L^{q}(Q)} \le \frac{\delta}{p} \|f\|_{L^{p}(Q)}^{p} + \frac{\delta^{-\frac{q}{p}}}{q} \|g\|_{L^{q}(Q)}^{q}.$$
(2.5a)

Poincaré-Friedrichs inequality, see [7], [6], [1]: Let $Q \subset \mathbb{R}^d$ be a parallelepiped (cuboid) and let the face $\Gamma \subset \partial Q$ vertical to the x_j , $1 \leq j \leq d$, coordinate plane. Then for any $f \in W^{1,p}(Q)$ with f = 0 on Γ , it holds

$$\int_{Q} |f|^{p} dx \leq C(Q) \sum_{1 \leq i \leq d} \int_{Q} |\partial_{x_{i}} f|^{p} dx.$$
(2.5b)

Let the vector $\boldsymbol{\beta} = (\beta_1, \dots, \beta_d)$, the function $f \in W^{1,p}(Q)$ and the outward normal vector **n** to ∂Q . In several places we will use the identities:

$$\nabla \cdot (\boldsymbol{\beta} f) = \boldsymbol{\beta} \cdot \nabla f + (\nabla \cdot \boldsymbol{\beta}) f, \qquad (2.6a)$$

$$2(\boldsymbol{\beta} \cdot \nabla f, f) = -(\nabla \cdot \boldsymbol{\beta} f, f) + 2 \int_{\partial Q} \boldsymbol{\beta} \cdot \mathbf{n} f^2 \, ds, \qquad (2.6b)$$

In what follows, positive constants c and C appearing in inequalities are generic constants which do not depend on the mesh-size h. In many cases, we will indicate on what may the constants depend for an easier understanding of the proofs. Frequently, we will write $a \leq b$ and $a \sim b$ meaning that $a \leq Cb$ and $c a \leq b \leq C a$ correspondingly, with generic positive constants c and C.

3 The parabolic quasilinear problem

Let Ω be a bounded cuboid domain in \mathbb{R}^{d_x} , with $d_x = 1, 2, 3$, with smooth boundary $\Gamma = \partial \Omega$. We define the space-time cylinder $\bar{Q} := \bar{\Omega} \times [0, T]$, where T is the final time, and boundary $\partial Q = \Sigma \cup \bar{\Sigma}_0 \cup \bar{\Sigma}_T$, where $\Sigma := \Gamma \times (0, T)$ is the lateral boundary, $\Sigma_0 := \Omega \times \{0\}$ and $\Sigma_T := \Omega \times \{T\}$. We consider the following quasilinear parabolic problem: find $u(x, t) : \bar{Q} \to \mathbb{R}$ such that

$$u_t - \operatorname{div} \mathbf{A}(\nabla_x u) = f \quad \text{in } Q \tag{3.1a}$$

$$u = u_{\Sigma} = 0 \text{ on } \Sigma, \tag{3.1b}$$

$$u(x,0) = u_0(x) \text{ on } \Omega, \qquad (3.1c)$$

where f, u_0 are given functions, and the function $\mathbf{A}(\mathbf{a}) : \mathbb{R}^{d_x} \to \mathbb{R}^{d_x}$ has the following p-power law form

$$\mathbf{A}(\mathbf{a}) = (\varepsilon + |\mathbf{a}|)^{p-2}\mathbf{a},\tag{3.2}$$

where p > 1 and $\varepsilon > 0$ are model parameters and |.| is the Euclidean norm. For simplifying the formulas below we introduce the notation

$$\alpha(\mathbf{a}) := (\varepsilon + |\mathbf{a}|)^{p-2}. \tag{3.3}$$

Next, we introduce several functions which will be useful to the rest parts of the text. For the vector **a**, the variable x > 0 and the parameter a, we define

$$\mathbf{F}(\mathbf{a}) = \left(\varepsilon + |\mathbf{a}|\right)^{\frac{p-2}{2}} \mathbf{a},\tag{3.4}$$

$$\varphi'(x) := (\varepsilon + x)^{p-2}x, \quad \frac{\varphi'_a(x)}{x} := \frac{\varphi'(a+x)}{a+x}$$
(3.5)

$$\varphi_a'(x) = (a + \varepsilon + x)^{p-2}x \tag{3.6}$$

$$\varphi(x) := \int_{0}^{\infty} \varphi'(s) ds = \int_{0}^{\infty} (\varepsilon + s)^{p-2} s ds$$
(3.7)

Remark 3.1. Note that for A as in (3.2) and φ' given in (3.5), it can be shown that $\varphi''(x)=(\varepsilon+x)^{p-3}(\varepsilon+(p-1)x) \ and \min\{1,p-1\}\leq (\varepsilon+x)^{p-2}\leq \varphi''(x)\leq p(\varepsilon+x)^{p-2}.$ This implies the equivalences $x\varphi'(x) \sim x^2 \varphi''(x) \sim (\varepsilon + x)^{p-2} x^2$.

Lemma 3.2 (Lemma 5.1 in [11]). Let \mathbf{A} be given by (3.2) and let \mathbf{F} be given by (3.4). Then the relations

$$(\mathbf{A}(\mathbf{P}) - \mathbf{A}(\mathbf{Q})) \cdot (\mathbf{P} - \mathbf{Q}) \sim |\mathbf{F}(\mathbf{P}) - \mathbf{F}(\mathbf{Q})|^2, \qquad (3.8a)$$

$$\sim \varphi_{|\mathbf{P}|} \left(|\mathbf{P} - \mathbf{Q}| \right),$$
 (3.8b)

$$\sim \varphi_{|\mathbf{Q}|} \left(|\mathbf{P} - \mathbf{Q}| \right),$$
 (3.8c)

$$\sim |\mathbf{P} - \mathbf{Q}|^2 \varphi'' (|\mathbf{P}| + |\mathbf{Q}|),$$
 (3.8d)

$$|\mathbf{A}(\mathbf{P}) - \mathbf{A}(\mathbf{Q})| \lesssim \varphi'' \left(|\mathbf{P}| + |\mathbf{Q}|\right) |\mathbf{P} - \mathbf{Q}|$$
(3.8e)

hold for all $\mathbf{P}, \mathbf{Q} \in \mathbb{R}^d$.

We will also recall the following lemma, proved in [11].

Lemma 3.3 (Lemma 6.2 in [11]). Let φ satisfy Assumption 5.1 in [11]. Then uniformly in $s, x \in \mathbb{R}$

$$\varphi''(|s| + |x|) |s - x| \sim \varphi'_{|s|}(|s - x|)$$

$$\varphi''(|s| + |x|) |s - x|^2 \sim \varphi_{|s|}(|s - x|).$$
(3.9)

Lemma 3.4 (Young's type inequality (Lemma 6.8 in [11])). Let φ be as in Definition 6.1 in [11]. Then for all $\delta > 0$ there exists c_{δ} such that for all $t, u, a \geq 0$

$$t\varphi_a'(u) + \varphi_a'(t)u \le \delta\varphi_a(t) + c_\delta\varphi_a(u)$$
(3.10)

Corollary 3.5. Let $u, v \in W^{1,p}(Q)$. Then by Lemma 3.2 and Lemma 3.3 we have that

$$\int_{Q} \left(\mathbf{A}(\nabla u) - \mathbf{A}(\nabla v) \right) \cdot \left(\nabla u - \nabla v \right) dx \, dt \sim \int_{Q} \left| \mathbf{F}(\nabla u) - \mathbf{F}(\nabla v) \right|^{2} dx dt \qquad (3.11)$$

$$\sim \int_{Q} \varphi_{|\nabla u|}(|\nabla u - \nabla v|) \, dx \, dt. \qquad (3.12)$$

Proposition 3.6. Let the real number $x \ge 0$ and the parameters $0 < \lambda < 1$ and $0 < \varepsilon \leq 1$. Then

$$\kappa x^2 - \left(\frac{1}{\varepsilon + x}\right)^{\lambda} x^2 \ge 0, \quad with \quad \kappa \ge \left(\frac{1}{\varepsilon}\right)^{\lambda},$$
(3.13a)

$$\left(\frac{1}{x}\right)^{\lambda}x^{2} - \kappa \left(\frac{1}{\varepsilon+x}\right)^{\lambda}x^{2} \le 0, \quad with \quad 1 < \kappa = \left(\frac{2}{\varepsilon}\right)^{\lambda+1},$$
 (3.13b)

Proof. Since $\frac{1}{\varepsilon} \ge \frac{1}{\varepsilon + x}$ for $x \ge 0$, (3.13a) follows directly. We consider $f : [0, \infty) \to \mathbb{R}$, $f(x) = \left(\frac{1}{x}\right)^{\lambda} x^2 - \kappa \left(\frac{1}{\varepsilon + x}\right)^{\lambda} x^2$ with f'(x) < 0 for all x > 0. Hence f is decreasing and $f(x) \le f(0) = 0$ and (3.13b) follows.

In next sections we derive the analysis for the case of $1 . In several places we add comments for the case <math>p \geq 2$, but this will be clearly written.

We first discuss some basic features of the solution of (3.1) and then we present approximations of the solution using space-time FE methods. We introduce appropriate stabilization terms in the design of the FE methods since a usual and direct application of FE to (3.1) can lead to numerical instabilities when the associated diffusion part of (3.1) is weak and the advection in time dominates.

3.1 Weak space-time form

We assume that $u_0 \in W^{1,p}(\Omega)$. Let $\boldsymbol{\ell} = (0,1)$ and $\mathbf{p} = (2,p)$. Following a standard procedure, we multiply (3.1) with a $v \in W^{1,\mathbf{p}}_{0,\overline{0}}(Q)$, see (2.4b), integrate with respect to both x and t, we derive the following space-time variational formulation: find $u \in W^{\boldsymbol{\ell},\mathbf{p}}_0(Q)$ such that

$$B^*(u,v) = \ell_f(v), \text{ for all } v \in W^{1,\mathbf{p}}_{0,\bar{0}}(Q),$$
 (3.14a)

with the bilinear form defined by

(3.14b)

$$B^*(u,v) = -\int_Q uv_t \, dx \, dt + \int_Q \alpha(\nabla_x u) \nabla_x u \cdot \nabla_x v \, dx \, dt, \qquad (3.14c)$$

and the linear form defined by

(3.14d)

$$\ell_f^*(v) = \int_Q f v \, dx \, dt + \int_\Omega u_0(x) v(x,0) \, dx. \tag{3.14e}$$

Last years, derivation of weak space-time formulations for parabolic evolution problems have been discussed in several works, see e.g., [22], [2], [24], [36]. For simplicity, we only consider homogeneous Dirichlet boundary conditions on Σ . However, the analysis presented in our paper can easily be generalized to other constellations of boundary conditions. The space-time variational formulation (3.14) has a unique solution, see, e.g., see [9], [36], and also [26], [37] for considerations in Gelfand triple spaces. In these works, beside existence and uniqueness results, one can also find useful a priori estimates and regularity results.

Assumption 1. We assume that the solution u of (3.14) belongs to $V = W_{\Sigma}^{1,p}(Q) \bigcap W^{\ell,p}(Q)$ with $\ell = (\ell_t, \ell_x), \ \ell_x \ge \ell_t = 2$, and $p > \frac{2d}{d+2}$. From (3.14) and Assumption 1 we can derive

$$B(u, v) = \ell_f(v), \text{ for all } v \in W^{1,\mathbf{p}}_{0,\bar{0}}(Q),$$
 (3.15a)

with

$$B(u,v) = \int_{Q} u_t v \, dx \, dt + \int_{Q} \alpha(\nabla_x u) \nabla_x u \cdot \nabla_x v \, dx \, dt \tag{3.15b}$$

$$\ell_f(v) = \int_Q f v \, dx \, dt \, dx. \tag{3.15c}$$

Note that $u(x,0) = u_0(x)$ in $L^2(\Omega)$ sense. Lets consider the case $u_0 = 0$. If we set u = v in (3.15), and then using (2.6b) and Lemma 3.2, we can deduce that

$$B(u,u) = \int_{\Sigma_{T}} \frac{1}{2} u^{2}(s) \, ds + \int_{Q} |\mathbf{F}(\nabla_{x}u)|^{2} \, dx \, dt$$

$$\lesssim \int_{Q} |fu| \, dx \, dt + \int_{\Omega} u_{0}^{2}(x) \, dx$$

$$\lesssim c(\delta) \int_{Q} |f|^{q} \, dx \, dt + \delta \int_{Q} |\nabla_{x}u|^{p} \, dx \, dt \qquad \left(\frac{1}{p} + \frac{1}{q} = 1\right) \qquad (3.16)$$

$$^{(3.13b)} \lesssim c(\delta) ||f||_{L^{q}(Q)}^{q} + \delta\kappa(\varepsilon, p) \int_{Q} \left(\varepsilon + |\nabla_{x}u|\right)^{p-2} |\nabla_{x}u|^{2} \, dx \, dt$$

$$\lesssim c(\delta) ||f||_{L^{q}(Q)}^{q} + \delta\kappa(\varepsilon, p) \int_{Q} |\mathbf{F}(\nabla_{x}u)|^{2} \, dx \, dt.$$

Choosing δ sufficiently small in (3.16), we can have the bound

$$\int_{\Sigma_T} u^2(s) \, ds + (1 - \delta \kappa(\varepsilon, p)) \int_Q |\mathbf{F}(\nabla_x u)|^2 \, dx \, dt \lesssim c(\delta) \|f\|_{L^q(Q)}^q. \tag{3.17}$$

Remark 3.7. Note that (3.17) does not provide a bound for controlling the variations of u_t . This indicates the importance of introducing appropriate stabilization terms in the numerical scheme, see (3.22) below.

Remark 3.8. After Assumption 1 maybe the usefulness of $W^{\ell,\mathbf{p}}$ spaces in (2.3) is not so clear. In the discretization error analysis below, different $L^{\mathbf{p}}$ norms will be used for estimating the temporal and the spatial parts of the error between the solution u and the space-time finite element solution u_h .

3.2 The space-time finite element approximation

We start by approximating (3.15) by stabilized finite element methods. Let $\mathcal{T}_h := \{E^i\}_{i=1,\dots,N}$ be a conforming mesh partition of the space-time cylinder Q into closed simplices (e.g., triangles or tetrahedra), such that

$$\bar{Q} = \bigcup_i E^i, \quad E^{\mathbf{o},i} \cap E^{\mathbf{o},j}, \ 1 \le i \ne j \le N,$$
(3.18)

where $E^{\circ,i}$ is the interior of the mesh element. The diameter of every $E^i \in \mathcal{T}_h$ is denoted by h_{E^i} and we set $h := \max_{E^i} h_{E^i}$. In the sequel we write $E \in \mathcal{T}_h$ instead of $E^i \in \mathcal{T}_h$. Assumption 2. The partition \mathcal{T}_h is quai-uniform, i.e., shape-regular and there is C_M independent of h such that $h \leq C_M h_E$ for $E \in \mathcal{T}_h$.

On \mathcal{T}_h we define the finite dimensional space

$$V_h^k = \{\phi_h \in C^0(\bar{Q}) : \phi_h|_E \in \mathbb{P}^k(E), \text{ for all } E \in \mathcal{T}_h, \text{ and } \phi_h = 0 \text{ on } \Sigma\}, \qquad (3.19)$$

here $\mathbb{P}^k(E)$ denotes the space of polynomials with degree less than or equal to $k \ge 1$ in E.

Assumption 3. For simplicity suppose that $u_0 = u_{0,h} := \prod_{h,L^2} (u_0)$, where \prod_{h,L^2} is the L^2 orthogonal projection onto V_h^k .

We now based on (3.15) consider the finite element problem: find $u_h \in V_h^k$ such that $u = u_{0,h}$ and

$$B(u_h, v_h) = \ell_f(v_h), \quad \text{for all} \quad v_h \in V_h^k.$$
(3.20)

In order to obtain stable solutions for the advection terms in t direction, the scheme (3.20) is modified by adding a stabilization term and the final stabilized scheme for the model problem is written: find $u_h \in V_h^k$ such that $u = u_{0,h}$ and

$$B_s(u_h, v_h) := B(u_h, v_h) + S(u_h, \partial_t v_h) = \ell_f(v_h + \tau^\lambda \partial_t v_h), \quad \text{for all} \quad v_h \in V_h^k, \quad (3.21)$$

where S has the form of streamline-upwind (SU)

$$S(u_h, \partial_t v_h) := \sum_{E \in \mathcal{T}_h} \int_E \tau^\lambda \partial_t u_h \partial_t v_h \, dx \, dt, \qquad (3.22)$$

here $\tau := \tau(h)$, and $0 < \lambda \leq 1 + \frac{d}{2} - \frac{d}{p}$ is a positive parameter to be specified below. **Remark 3.9.** The function $w_h = v_h + \tau^\lambda \partial_t v_h$ satisfies $w_h = 0$ on Σ .

Remark 3.10. Based on Assumption 1, we can write the following localized variational form for the weak solution u

$$B_s(u, v_h) := B(u, v_h) + S(u, \partial_t v_h) = \ell_f(v_h + \tau^\lambda \partial_t v_h), \quad \text{for all} \quad v_h \in V_h^k, \quad (3.23)$$

or in analytical expression

$$B_{s}(u, v_{h}) := \sum_{E \in \mathcal{T}_{h}} \int_{E} \partial_{t} u v_{h} + \mathbf{A}(\nabla_{x} u) \cdot \nabla_{x} v_{h} \, dx \, dt + \sum_{E \in \mathcal{T}_{h}} \int_{E} \tau^{\lambda} \partial_{t} u \, \partial_{t} v_{h} \, dx \, dt,$$

$$\ell_{f}(v_{h}) := \sum_{E \in \mathcal{T}_{h}} \int_{E} f\left(v_{h} + \tau^{\lambda} \partial_{t} v_{h}\right) dx dt.$$
(3.24)

Note that the form $B_s(\cdot, \cdot)$ is linear in the second argument. In view of (3.23), we have the following equation.

Corollary 3.11. Let the solution u of problem (3.15a) and the solution u_h of problem (3.21). Then the following error equation holds

$$B_s(u, v_h) - B_s(u_h, v_h) = 0, \quad for \quad v_h \in V_h^k.$$
 (3.25)

Proposition 3.12. Let $v_h \in V_h^k$ and $u_0 = 0$. Then

$$B_{s}(v_{h}, v_{h}) \geq \frac{1}{2} \|v\|_{L^{2}(\Sigma_{T})}^{2} + \sum_{E \in \mathcal{T}_{h}} \tau^{\lambda} \|\partial_{t} v_{h}\|_{L^{2}(E)}^{2} + c_{e} \|\mathbf{F}(\nabla_{x} v_{h})\|_{L^{2}(Q)}^{2}, \qquad (3.26)$$

where c_e is the constant appearing in (3.8).

Proof. For $E \in \mathcal{T}_h$ denote the unit normal vector on ∂E by $\mathbf{n}_E = (n_{x,E}, n_{t,E})$, and the unit normal vector on the common faces $F_{ij} = \partial E^i \cap \partial E^j$ for $E^i, E^j \in \mathcal{T}_h$ by $\mathbf{n}_{ij} = (n_{x,ij}, n_{t,ij})$. Using (2.6b) it follows immediately that

$$\sum_{E \in \mathcal{T}_{h}} \int_{E} \partial_{t} v_{h} v_{h} \, dx \, dt = \frac{1}{2} \sum_{E \in \mathcal{T}_{h}} \int_{E} \partial_{t} v_{h}^{2} \, dx \, dt$$

$$= \frac{1}{2} \sum_{E \in \mathcal{T}_{h}} \int_{\partial E} n_{t,E} v_{h}^{2} dS = \frac{1}{2} \sum_{F_{ij}} \int_{F_{ij}} n_{t,ij} \left(v_{h}^{2} |_{E^{i}} - v_{h}^{2} |_{E^{j}} \right) dS = \frac{1}{2} \int_{\Sigma_{T}} v_{h}^{2} dS. \quad (3.27)$$

By the definition of $B_s(\cdot, \cdot)$ and (3.8a) we have that

$$B_{s}(v_{h}, v_{h}) = \sum_{E \in \mathcal{T}_{h}} \int_{E} \left[\partial_{t} v_{h} v_{h} + \tau^{\lambda} \left(\partial_{t} v_{h} \right)^{2} + \mathbf{A} (\nabla_{x} v_{h}) \cdot \nabla_{x} v_{h} \right] dx dt,$$

$$\geq \frac{1}{2} \| v \|_{L^{2}(\Sigma_{T})}^{2} + \sum_{E \in \mathcal{T}_{h}} \tau^{\lambda} \| \partial_{t} v_{h} \|_{L^{2}(E)}^{2} + c_{e} \| \mathbf{F} (\nabla_{x} v_{h}) \|_{L^{2}(Q)}^{2}.$$
(3.28)

Taking into consideration (3.16) and (3.26), for $v \in V + V_h^k$ we introduce the mesh-dependent norms

$$\|v\|_{h}^{2} := \frac{1}{2} \|v\|_{L^{2}(\Sigma_{T})}^{2} + \sum_{E \in \mathcal{T}_{h}} \tau^{\lambda} \|\partial_{t}v\|_{L^{2}(E)}^{2} + \|\mathbf{F}(\nabla_{x}v)\|_{L^{2}(Q)}^{2}, \qquad (3.29a)$$

$$\|v\|_{h,*}^{2} := \|v\|_{h}^{2} + \sum_{E \in \mathcal{T}_{h}} \tau^{-\lambda} \|\partial_{t}v\|_{L^{2}(E)}^{2}.$$
(3.29b)

Lemma 3.13. Let D be a bounded domain in \mathbb{R}^d , and the integers $j \ge 0$ and $\ell = j+1$. Let the function $v \in W^{\ell,p}(D)$ with $p \ge \frac{2d}{d+2}$. Then it holds, [1],

$$\|v\|_{W^{j,2}(D)} \le C_{\ell,p,Q} \|v\|_{W^{\ell,p}(D)}.$$
(3.30)

Lemma 3.14. The embedding relation (3.30) implies the following scaling relation

$$h^{\frac{-d}{2}} \|v\|_{L^{2}(E)} \lesssim h^{\frac{-d}{p}} \left(\|v\|_{L^{p}(E)}^{p} + h^{p} \|\partial_{t}v\|_{L^{p}(E)}^{p} + h^{p} \|\nabla_{x}v\|_{L^{p}(E)}^{p} \right)^{\frac{1}{p}}, \quad E \in \mathcal{T}_{h}.$$
(3.31)

Proof. See proof and discussion in [7], see also [21].

Lemma 3.15. Let u the weak solution of (3.15) under Assumption 1 and $u_0 = 0$. Let $u_h \in V_h^k$ be the finite element solution in (3.20). The approximation error estimate

$$c_{0,min} \|u - u_h\|_h^2 \le C_{0,Max} \|u - v_h\|_{h,*}^2,$$
(3.32)

holds for all $v_h \in V_h^k$, where the constants $c_{0,min}$ and $C_{0,Max}$ are independent of h.

Proof. Recalling (3.25) we have that

$$B_{s}(u, u - u_{h}) - B_{s}(u_{h}, u - u_{h}) = B_{s}(u, u) - B_{s}(u, u_{h}) - B_{s}(u_{h}, u) + B_{s}(u_{h}, u_{h})$$

$$= B_{s}(u, u) - B_{s}(u, v_{h}) - B_{s}(u_{h}, u) + B_{s}(u_{h}, v_{h})$$

$$= B_{s}(u, u - v_{h}) - B_{s}(u_{h}, u - v_{h}).$$
(3.33)

Using (3.24) we obtain the following representation for the left hand side in (3.33)

$$B_{s}(u, u - u_{h}) - B_{s}(u_{h}, u - u_{h})$$

$$= \sum_{E \in \mathcal{T}_{h}} \int_{E} \left[(\partial_{t}u - \partial_{t}u_{h}) (u - u_{h}) + \tau^{\lambda} (\partial_{t}u - \partial_{t}u_{h})^{2} \right] dxdt$$

$$+ \sum_{E \in \mathcal{T}_{h}} \int_{E} \left[(A(\nabla_{x}u) - A(\nabla_{x}u_{h})) (\nabla_{x}u - \nabla_{x}u_{h}) dx dt.$$
(3.34)

In similar way the right hand side in (3.33) is equivalent to

$$B_{s}(u, u - v_{h}) - B_{s}(u_{h}, u - v_{h})$$

$$= \sum_{E \in \mathcal{T}_{h}} \int_{E} \left[(\partial_{t}u - \partial_{t}u_{h}) (u - v_{h}) + \tau^{\frac{\lambda}{2}} (\partial_{t}u - \partial_{t}u_{h}) \tau^{\frac{\lambda}{2}} (\partial_{t}u - \partial_{t}v_{h}) \right] dxdt$$

$$+ \sum_{E \in \mathcal{T}_{h}} \int_{E} \left[(A(\nabla_{x}u) - A(\nabla_{x}u_{h})) \cdot (\nabla_{x}u - \nabla_{x}v_{h}) dx dt.$$
(3.35)

Inserting (3.34) and (3.35) in to (3.33) and then making use of (2.6b) and (3.8b) we derive

$$\frac{1}{2} \|u - u_h\|_{L^2(\Sigma_T)}^2 + c_1 \int_Q \varphi_{|\nabla_x u|} \left(|\nabla_x u - \nabla_x u_h| \right) dx dt + \sum_{E \in \mathcal{T}_h} \int_E \left[\tau^\lambda \left(\partial_t u - \partial_t u_h \right)^2 \right] dx dt \\
\leq B_s(u, u - u_h) - B_s(u_h, u - u_h) \\
= B_s(u, u - v_h) - B_s(u_h, u - v_h) \\
= \int_Q \left(\partial_t u - \partial_t u_h \right) (u - v_h) dx dt \\
+ \sum_{E \in \mathcal{T}_h} \int_E \tau^{\frac{\lambda}{2}} \left(\partial_t u - \partial_t u_h \right) \tau^{\frac{\lambda}{2}} \left(\partial_t u - \partial_t v_h \right) dx dt \\
+ \int_Q \left(A(\nabla_x u) - A(\nabla_x u_h) \right) \cdot \left(\nabla_x u - \nabla_x v_h \right) dx dt \\
= T_1 + T_2 + T_3.$$
(3.36)

We now estimate the term T_1 on the right hand side in (3.36). We perform integration

by parts and then apply (2.5a) to get

$$T_{1} = \int_{Q} (\partial_{t}u - \partial_{t}u_{h}) (u - v_{h}) dx dt = -\int_{Q} (u - u_{h}) (\partial_{t}u - \partial_{t}v_{h}) dx dt + \int_{\Sigma_{T}} (u - u_{h}) (u - v_{h}) dx - \underbrace{\int_{\Sigma_{0}} (u - u_{h}) (u - v_{h}) dx}_{=0} \leq \tau^{\frac{\lambda}{2}} \|u - u_{h}\|_{L^{2}(Q)} \tau^{-\frac{\lambda}{2}} \|\partial_{t}u - \partial_{t}v_{h}\|_{L^{2}(Q)} + \|u - u_{h}\|_{L^{2}(\Sigma_{T})} \|u - v_{h}\|_{L^{2}(\Sigma)} by (2.5b) \leq C\tau^{\frac{\lambda}{2}} \|\partial_{t}u - \partial_{t}u_{h}\|_{L^{2}(Q)} \tau^{-\frac{\lambda}{2}} \|\partial_{t}u - \partial_{t}v_{h}\|_{L^{2}(Q)} + \|u - u_{h}\|_{L^{2}(\Sigma_{T})} \|u - v_{h}\|_{L^{2}(\Sigma)} \leq C\frac{\delta_{1}}{2} \tau^{\lambda} \|\partial_{t}u - \partial_{t}u_{h}\|_{L^{2}(Q)}^{2} + c(\delta_{1})\tau^{-\lambda} \|\partial_{t}u - \partial_{t}v_{h}\|_{L^{2}(Q)}^{2} + \frac{\delta_{2}}{2} \|u - u_{h}\|_{L^{2}(\Sigma_{T})}^{2} + c(\delta_{2})\|u - v_{h}\|_{L^{2}(\Sigma_{T})}^{2},$$

$$(3.37)$$

where the parameters $\delta_1 > 0$ and $\delta_2 > 0$ are sufficiently small. For the next term

$$T_{2} = \sum_{E \in \mathcal{T}_{h}} \int_{E} \tau^{\frac{\lambda}{2}} |\partial_{t}u - \partial_{t}u_{h}| \tau^{\frac{\lambda}{2}} |\partial_{t}u - \partial_{t}v_{h}| \, dx \, dt$$

$$\leq \left(\sum_{E \in \mathcal{T}_{h}} \tau^{\lambda} ||\partial_{t}u - \partial_{t}u_{h}||^{2}_{L^{2}(E)} \right)^{\frac{1}{2}} \left(\sum_{E \in \mathcal{T}_{h}} \tau^{\lambda} ||\partial_{t}u - \partial_{t}v_{h}||^{2}_{L^{2}(E)} \right)^{\frac{1}{2}} \qquad (3.38)$$

$$\leq \delta_{0} \left(\sum_{E \in \mathcal{T}_{h}} \tau^{\lambda} ||\partial_{t}u - \partial_{t}u_{h}||^{2}_{L^{2}(E)} \right) + C_{\delta_{0}} \left(\sum_{E \in \mathcal{T}_{h}} \tau^{\lambda} ||\partial_{t}u - \partial_{t}v_{h}||^{2}_{L^{2}(E)} \right),$$

where $\delta_0 > 0$ is a small number will be appropriately chosen below. For the term T_3 we work as follows: we use Lemma 3.2 and Lemma 3.3, and then the fact that $\varphi'(s) \sim s\varphi''(s)$, see Remark 3.1, to obtain

$$T_{3} \leq \int_{Q} \varphi'_{|\nabla_{x}u|} \left(|\nabla_{x}u - \nabla_{x}u_{h}| \right) |\nabla_{x}u - \nabla_{x}v_{h}| \, dxdt$$

$$\leq \delta_{3} \int_{Q} \varphi_{|\nabla_{x}u|} \left(|\nabla_{x}u - \nabla_{x}u_{h}| \right) \, dx \, dt + c_{\delta_{3}} \int_{Q} \varphi_{|\nabla_{x}u|} \left(|\nabla_{x}u - \nabla_{x}v_{h}| \right) \, dx \, dt$$

$$\leq c_{4}\delta_{3} \int_{Q} |\mathbf{F}(\nabla_{x}u) - \mathbf{F}(\nabla_{x}u_{h})|^{2} \, dxdt + c_{4}c_{\delta_{3}} \int_{Q} |\mathbf{F}(\nabla_{x}u) - \mathbf{F}(\nabla_{x}v_{h})|^{2} \, dxdt,$$

(3.39)

where in the last step above the relations (3.8a) and (3.8b) have been used. Making again use of (3.8a) and (3.8b) we also have

$$c_{3} \int_{Q} \left| \mathbf{F}(\nabla_{x} u) - \mathbf{F}(\nabla_{x} u_{h}) \right|^{2} dx dt \leq \int_{Q} \varphi_{|\nabla_{x} u|} \left(\left| \nabla_{x} u - \nabla_{x} u_{h} \right| \right) dx dt$$
(3.40)

We introduce (3.37), (3.38), (3.39) and (3.40) in to (3.36) to obtain the bound

$$\left(\frac{1-\delta_2}{2}\right) \|u-u_h\|_{L^2(\Sigma_T)}^2 + C_{P,0}\left(1-\frac{\delta_0+\delta_1}{2}\right) \left(\sum_{E\in\mathcal{T}_h}\tau^\lambda \|\partial_t u - \partial_t u_h\|_{L^2(E)}^2\right)
+ \left(c_1c_3 - \delta_3c_2c_4\right) \int_Q |\mathbf{F}(\nabla_x u) - \mathbf{F}(\nabla_x u_h)|^2 dxdt
\leq c(\delta_1)\tau^{-\lambda} \|\partial_t u - \partial_t v_h\|_{L^2(Q)}^2 + c(\delta_2) \|u-v_h\|_{L^2(\Sigma_T)}^2
+ C_{\delta_0}\left(\sum_{E\in\mathcal{T}_h}\tau^\lambda \|\partial_t u - \partial_t v_h\|_{L^2(E)}^2\right) + c_2c_4c_{\delta_3}\int_Q |\mathbf{F}(\nabla_x u) - \mathbf{F}(\nabla_x v_h)|^2 dxdt.$$
(3.41)

Choosing in above inequality the numbers δ_i , i = 0, 1, 2, 3 sufficiently small such that all the constants to be positive, we obtain

$$c_{\delta_{2}} \|u - u_{h}\|_{L^{2}(\Sigma_{T})}^{2} + c_{\delta_{0},\delta_{1}} \Big(\sum_{E \in \mathcal{T}_{h}} \tau^{\lambda} \|\partial_{t}u - \partial_{t}u_{h}\|_{L^{2}(E)}^{2} \Big)$$

$$+ c_{\delta_{3}} \int_{Q} |\mathbf{F}(\nabla_{x}u) - \mathbf{F}(\nabla_{x}u_{h})|^{2} dx dt$$

$$\leq C_{\delta_{1}} \tau^{-\lambda} \|\partial_{t}u - \partial_{t}v_{h}\|_{L^{2}(Q)}^{2} + C_{\delta_{2}} \|u - v_{h}\|_{L^{2}(\Sigma_{T})}^{2}$$

$$+ C_{\delta_{0}} \Big(\sum_{E \in \mathcal{T}_{h}} \tau^{\lambda} \|\partial_{t}u - \partial_{t}v_{h}\|_{L^{2}(E)}^{2} \Big) + C_{\delta_{3}} \int_{Q} |\mathbf{F}(\nabla_{x}u) - \mathbf{F}(\nabla_{x}v_{h})|^{2} dx dt.$$

$$(3.42)$$

Finally, choosing $c_{0,min} = \min\{c_{\delta_2}, c_{\delta_0,\delta_1}, c_{\delta_3}\}$ and $C_{0,Max} = \max\{C_{\delta_1}, C_{\delta_2}, C_{\delta_0}, C_{\delta_3}\}$, we can have the desired estimate.

Corollary 3.16. Let the solutions u and u_h satisfy the assumptions of Lemma 3.15. Then the approximation error estimate

$$\|u - u_h\|_{L^2(\Sigma_T)}^2 + \tau^{\lambda} \|\mathbf{F}(\partial_t u) - \mathbf{F}(\partial_t u_h)\|_{L^2(Q)}^2 + \|\mathbf{F}(\nabla_x u) - \mathbf{F}(\nabla_x u_h)\|_{L^2(Q)} \le C_{0,\mathbf{F}}^* \|u - v_h\|_{h,*}^2,$$
(3.43)

holds for all $v_h \in V_h^k$ where the constant is independent of h.

Proof. In view of (3.13a) we can have

$$0 < \int_{E} \varphi''(|\partial_{t}u| + |\partial_{t}u_{h}|)||\partial_{t}u - \partial_{t}u_{h}|^{2} dx dt \le C_{\varepsilon} \int_{E} |\partial_{t}u - \partial_{t}u_{h}|^{2} dx dt \qquad (3.44)$$

for an appropriate constant C_{ε} . Now this inequality combined with (3.8d) gives

$$\sum_{E \in \mathcal{T}_h} \int_E |\partial_t u - \partial_t u_h|^2 \, dx \, dt \gtrsim \sum_{E \in \mathcal{T}_h} \int_E |\mathbf{F}(\partial_t u) - \mathbf{F}(\partial_t u_h)|^2 \, dx \, dt.$$
(3.45)

Finally, (3.43) follows by introducing (3.45) into (3.42) and rearranging appropriately the constants.

In Section Appendix, similar approximation error estimates as those in (3.32) and (3.43) are given for $p \ge 2$, see Remark 5.1.

Note that the error estimates (3.32) and (3.43) include bounds for the term $\|\partial_t u \partial_t u_h \|_{L^2}$, which is associated with the time discretization, compare with Remark 3.7 and Remark 3.8.

Using Sobolev embedding relations, see [1], Assumption 1 implies that $u \in W^{1+s_p,2}(Q)$ with $s_p = \frac{d+2}{2} - \frac{d}{p} > 0$. Let $\Pi_h : V \to V_h^1$ be an interpolation operator, e.g., Scott-Zhang, [7], we have the following interpolation error estimates.

Lemma 3.17. Let the function $v \in V$ with $\ell_x \geq \ell_t = 2$, see Assumption 1, such that $\ell_t > d/p$, furthermore let Assumption 2 for the mesh \mathcal{T}_h . Then the interpolation estimates

$$v - \prod_{h} v|_{W^{1,p}(Q)} \le c_{intp,p} h^{(\ell_t - 1)} \|v\|_{W^{\ell_t,p}(Q)}, \qquad (3.46a)$$

$$\begin{aligned} v - \Pi_h v|_{W^{1,p}(Q)} &\leq c_{intp,p} h^{(\ell_t - 1)} \|v\|_{W^{\ell_t,p}(Q)}, \\ \|v - \Pi_h v\|_{L^2(Q)} &\leq c_{intp,0} h^{1 + s_p} \|v\|_{W^{2,p}(Q)}, \end{aligned}$$
(3.46a) (3.46b)

$$|v - \Pi_h v|_{W^{1,2}(Q)} \le c_{intp,1} h^{s_p} ||v||_{W^{2,p}(Q)}, \qquad (3.46c)$$

$$\|\mathbf{F}(\nabla v) - \mathbf{F}(\nabla \Pi_h v)\|_{L^2(Q)} \le c_{intp,F} h^{(\ell_t - 1)\frac{\nu}{2}} \|v\|_{W^{\ell_t, p}(Q)},$$
(3.46d)

hold with the constants $c_{intp,p}$, $c_{intp,0}$, $c_{intp,1} c_{intp,F}$ are independent of h.

Proof. For the interpolation estimate (3.46a) we refer to [7]. Next we prove directly the estimate (3.46b). The estimate (3.46c) can be shown in similar way. The relation (3.31) implies that

$$\left(\sum_{E\in\mathcal{T}_{h}}\|v-\Pi_{h}v\|_{L^{2}(E)}^{2}\right)^{\frac{1}{2}} \lesssim \left(\sum_{E\in\mathcal{T}_{h}}h^{2\left(-\frac{d}{p}+\frac{d}{2}\right)}\left(\|v-\Pi_{h}v\|_{L^{p}(E)}^{p}+h^{p}\|\nabla v-\nabla\Pi_{h}v\|_{L^{p}(E)}^{p}\right)^{\frac{1}{2}} \\ \lesssim h^{-\frac{d}{p}+\frac{d}{2}}\left(\sum_{E\in\mathcal{T}_{h}}\left(\|v-\Pi_{h}v\|_{L^{p}(E)}^{2}+h^{2}\|\nabla v-\nabla\Pi_{h}v\|_{L^{p}(E)}^{2}\right)\right)^{\frac{1}{2}} \\ \lesssim (\text{observe that } f(x) = (a^{x}+b^{x})^{\frac{1}{x}} \downarrow \text{ for } a, b > 0 \text{ and using that } 1$$

The proof of (3.46d) is given in [25].

Let a mesh element $E \in \mathcal{T}_h$ and let a function $v \in W^{1,p}(Q)$. Then, it is known, (cf. [7]), that there is a constant $C_{trc} > 0$, such that

$$\|v\|_{L^{p}(\partial E)}^{p} \leq C_{trc}h^{-1}(\|v\|_{L^{p}(E)} + h\|\nabla v\|_{L^{p}(E)})^{p}.$$
(3.48)

We now return to the question of the convergence of the finite element solution u_h defined in (3.21). We need the following quasi-interpolation estimate.

Lemma 3.18. Let $v \in V$ satisfying the assumptions of Lemma 3.17, and let the associated interpolant $\Pi_h v$, see (3.46). Then there exist a constant independent of v and h such that the following quasi-interpolation estimate

$$\|v - \Pi_h v\|_{h,*}^2 \lesssim \left(h^{1+2s_p} + \tau^{\lambda} h^{2s_p} + h^p + \tau^{-\lambda} h^{2s_p}\right) \left(\|\mathbf{F}(v)\|_{W^{1,2}(Q)}^2 + \|v\|_{W^{2,p}(Q)}^2\right),$$
(3.49)

holds true.

Proof. Recall that

$$\|v\|_{h,*}^{2} = \frac{1}{2} \|v\|_{L^{2}(\Sigma_{T})}^{2} + \sum_{E \in \mathcal{T}_{h}} \tau^{\lambda} \|\partial_{t}v\|_{L^{2}(E)}^{2} + \|\mathbf{F}(\nabla_{x}v)\|_{L^{2}(Q)}^{2} + \sum_{E \in \mathcal{T}_{h}} \tau^{-\lambda} \|\partial_{t}v\|_{L^{2}(E)}^{2}.$$
(3.50)

Under the regularity assumptions and by applying (3.46) and (3.48) we have the following estimates

$$\frac{1}{2} \|v - \Pi_h v\|_{L^2(\Sigma_T)}^2 \leq Ch^{-1} \left(\|v - \Pi_h v\|_{L^2(Q)} + h \|\nabla v - \nabla \Pi_h v\|_{L^2(Q)} \right)^2 \\
\leq Ch^{-1} \left(c_{intp,0} h^{1+s_p} + c_{intp,1} h^{1+s_p} \right)^2 \|v\|_{W^{2,p}(Q)}^2 \\
\lesssim h^{1+2s_p} \|v\|_{W^{2,p}(Q)}^2,$$

and also

$$\sum_{E\in\mathcal{T}_h}\tau^{\pm\lambda}\|\partial_t v - \partial_t\Pi_h v\|_{L^2(E)}^2 \leq \tau^{\pm\lambda}|\nabla v - \nabla\Pi_h v|_{L^2(Q)}^2 \lesssim \tau^{\pm\lambda}h^{2s_p}\|v\|_{W^{2,p}(Q)}^2.$$

Using (3.46) and the previous estimates in (3.50) we derive (3.49).

Theorem 3.19. Let the solutions u and u_h satisfy the assumptions in Lemma 3.15 and let the Π_h satisfy the assumptions in Lemma 3.17. Then the following error convergence result holds

$$\|u - u_h\|_h^2 \lesssim \tau^{-\lambda} h^{2s_p} \big(\|\mathbf{F}(u)\|_{W^{1,2}(Q)}^2 + \|u\|_{W^{2,p}(Q)}^2 \big).$$
(3.51)

Proof. We recall that $0 < \lambda \leq s_p = 1 + \frac{d}{2} - \frac{d}{p}$. Then, we combine Lemma 3.15 and Lemma 3.18 and the assertion follows.

One can alternatively use the following result and to derive analogous interpolation estimates as those in (3.46) and in (3.49).

Lemma 3.20. The following estimate

$$\|\nabla_x u - \nabla_x \Pi_h u\|_{L^p(Q)} \le c_*(u) \Big(\int_Q |\mathbf{F}(\nabla_x u) - \mathbf{F}(\nabla_x \Pi_h u)|^2 \, dx \, dt\Big)^{\frac{1}{2}} \tag{3.52}$$

holds for a constant $c_*(u) > 0$.

Proof. The proof is given in Section Appendix.

Note that estimate (3.52) can be extended and used under different regularity assumptions, i.e., $\mathbf{F}(\nabla u) \in W^{1,2}$. This can be further connected with the analysis presented in [11] and in [10] for showing unified convergence estimates with respect to time and to space for the space-time FE method in (3.21). A work in this direction is a subject of current research.

4 Numerical Examples

In order to validate the estimates derived in the previous sections, we now perform a series of numerical tests choosing different values for the parameters of the problem. We set $\tau = 0.2h^{\lambda}$ with $\lambda = \frac{1}{2}s_p$ when $u \in W^{2,p}$ and $\lambda = \frac{1}{2}$ when the solution $u \in W^{2,2}$. First we start by considering the problem on a space time cylinder $Q \subset \mathbb{R}^2$ with smooth solution and then with less regular solution. Thereafter we present computations considering the problem on $Q \subset \mathbb{R}^3$. During the error analysis we used different $L^{\mathbf{p}}$ -norms for the variations of the error in time and space direction. This helped in some way on having a different treatment on the estimation of the two parts of the global error, where the one is related to the time discretization and the other is related to the space discretization. A complete separation of the error parts and an individual computation of their estimates seems not to be obvious. However, looking into the proof of the error estimate (3.32), we can see that the dominated bound is mainly related to $\tau^{-\lambda} \|\partial_t u - \partial_t v_h\|_{L^2}^2$. We can therefore expect that the asymptotic converge of $\tau^{\lambda} \|\partial_t u - \partial_t u_h\|_{L^2}^2$ is going to be determined by the approximation error $\tau^{-\lambda} \|\partial_t u - \partial_t v_h\|_{L^2}^2$, and correspondingly the behavior of $\|\mathbf{F}(\nabla_x u) - \mathbf{F}(\nabla_x u_h)\|_{L^2}$ is going to be determined by $\tau^{-\lambda} \|\partial_t u - \partial_t v_h\|_{L^2}^2 + \|\mathbf{F}(\nabla_x u) - \mathbf{F}(\nabla_x v_h)\|_{L^2}^2$, see Lemma 3.17 and Lemma 3.18. In the numerical examples below we investigate the asymptotic convergence behavior of the whole error $||u - u_h||_h$, as well of the error parts $\|\partial_t u - \partial_t u_h\|_{L^2}$ and $\|\mathbf{F}(\nabla_x u) - \mathbf{F}(\nabla_x u_h)\|_{L^2}$. The examples have been solved on a series of uniform mesh refinement levels with $h_s, h_{s+1}, ...,$ using first order (k = 1, ..., k = 1)see (3.19)) local polynomial spaces. In any computational case, the asymptotic convergence rates are computed by the ratio $ln(e_s/e_{s+1})/ln(h_s/h_{s+1})$, where e_s is the corresponding error which is written in the table columns. Our goal is mainly to study the behavior of the convergence rates $r_t^{L^2}$ and $r_{F,t}$ of the errors $\|\partial_t u - \partial_t u_h\|_{L^2}$ and $\|\mathbf{F}(\partial_t u) - \mathbf{F}(\partial_t u_h)\|_{L^2}$. The "expected values" of the rates which are written in the tables have been computed using Lemma 3.15, Lemma 3.17 and Theorem 3.19. Based on Corollary 3.16 and Proposition 5.2 the behavior of $r_t^{L^2}$ and $r_{F,t}$ is expected to be very similar.

For the solution of the resulting non-linear system a Picard iterative scheme is applied. For all numerical tests the iterative scheme meets the convergence criteria in (maximum) seven iterations. For the solution of the linear scheme a direct LU method is used. More sophisticated nonlinear iterative methods for *p*-Laplace problems are discussed in [34]. All tests have been computed using FreeFem++ library¹.

Note that we developed the analysis in the previous sections by considering that $u_{\Sigma} = 0$, see (3.1). Anyway, in the numerical computations the initial condition u_0 and the boundary data u_{Σ} are determined by the L^2 -projection of the exact solution u onto polynomial space.

The conclusion from the results presented below is that the proposed space-time FE scheme behaves well for each *p*-value that we choose. In each case the numerical convergence rates are in agreement with the theoretical predicted rates, and for some cases slightly better.

¹http://www3.freefem.org/

4.1 Examples in two-dimensional space-time cylinders

Smooth test case In the first numerical example the domain is $\bar{Q} = [0:0.4] \times [0:0.4]$ and the exact solution is $u(x,t) = ((x-0.2)^2 + (t-0.2)^2)^{\frac{\gamma}{2}}$ with $\gamma = 2 + \frac{2}{p}$. The problem has been solved for $p \in \{1.15, 1.25, 1.5\}$ setting $\varepsilon = 1$. For all *p*-test cases the associated solution is smooth and we have $\lambda = \frac{1}{2}$. Thus the expected convergence rates are $r_t^{L^2} = 0.5$, $r_{F,t} = 0.5$ and $r_{F,x} = 0.75$. In Table 1 we display the results of the asymptotic convergence rates of all *p*-cases. We observe that the rates $r_t^{L^2}$ and $r_{F,t}$ have similar behavior and are little higher than the expected rates, but progressively as the meshes are refined, both $r_t^{L^2}$ and $r_{F,t}$ tend to the expected values. In the last columns we can see the rates $r_{F,x}$ of $\|\mathbf{F}(\nabla_x u) - \mathbf{F}(\nabla_x u_h)\|_{L^2}$. For each *p*-case the rates have high values on the first coarse meshes. Moving to the finer meshes the values reduce down to the expected values.

$u \in W^{\ell \ge 2,2}(Q) \text{ with } u(x,t) = ((x-0.2)^2 + (t-0.2)^2)^{\frac{\gamma}{2}}, \varepsilon = 1,$									
errors	$\ \partial_t u - \partial_t u_h\ _{L^2}$			$\ \mathbf{F}(\partial_t u) - \mathbf{F}(\partial_t u_h)\ _{L^2}$			$\ \mathbf{F}(\nabla_x u) - \mathbf{F}(\nabla_x u_h)\ _{L^2}$		
$\mathbf{p}:=$	p=1.15	p=1.25	p=1.5	p=1.15	p=1.25	p=1.5	p=1.15	p=1.25	p=1.5
expected rates	0.5	0.50	0.5	0.5	0.5	0.5	0.75	0.75	0.75
$h_0 = 0.2$				Con	nputed ra	tes			
$h_s = \frac{h_0}{2^s}$	$r_t^{L^2}$	$r_t^{L^2}$	$r_t^{L^2}$	$r_{F,t}$	$r_{F,t}$	$r_{F,t}$	$r_{F,x}$	$r_{F,x}$	$r_{F,x}$
s = 0	-	-	-	-	-		-	-	-
s = 1	0.5354	0.59505	0.6568	0.5867	0.6097	0.6379	0.7047	7189	0.7303
s=2	0.8708	0.8424	0.8771	0.8253	0.8424	0.8771	1.0165	0.9423	0.8193
s = 3	0.9958	0.9624	0.9713	0.9801	0.9624	0.9713	0.9916	1.0160	1.0146
s = 4	0.9554	0.9824	0.9866	0.9718	0.9824	0.9866	0.9953	0.9970	1.0008
s = 5	0.8719	0.9751	0.9813	0.9306	0.9751	0.9813	0.9782	0.9825	0.9898
s = 6	0.7367	0.9386	0.9537	0.7349	0.9386	0.9537	0.9544	0.9626	0.9765
s = 7	0.6276	0.7401	0.8757	0.6218	0.7401	0.8757	0.9155	0.9293	0.9538
s = 8	0.6015	0.5764	0.6324	0.6025	0.5764	0.6324	0.8554	0.8759	0.9150
s = 9	0.5141	0.5357	0.5868	0.5141	0.5357	0.5868	0.7761	0.8014	0.8547

Table 1: Example 1: smooth test case. The convergence rates $r_t^{L^2}$ and $r_{F,t}$ and $r_{F,x}$.

Point singularity test case We consider the problem on $\bar{Q} = [0:0.4] \times [0:0.4]$ with exact solution $u(x,t) = ((x-0.2)^2 + (t-0.2)^2)^{\frac{\gamma}{2}}$ with $\gamma = 2.1 - \frac{2}{p}$. The problem has been solved for $p \in \{1.15, 1.25, 1.5\}$ setting $\varepsilon = 1$. Note that the singular point of the solution is located at the center of the domain. For all the *p*-test cases the associated solution *u* belongs to $W^{2,p}(Q)$, and thus according to Lemma 3.15 and Theorem 3.19 the values of $r_t^{L^2}$, $r_{F,t}$ are expected to be close to $\frac{s_p}{2}$, and the values of $r_{\parallel,\parallel_h}$ close to $\frac{3}{4}s_p$. We compute the rates on a sequence of meshes and we present the results in Table 2. Looking at the table, we observe that for the p = 1.15 and p = 1.25 tests, the rates related to $\|\partial_t u - \partial_t u_h\|_{L^2}$ and $\|\mathbf{F}(\partial_t u) - \mathbf{F}(\partial_t u_h)\|_{L^2}$ are close to the expected values even from the first mesh refinement steps. For the third p = 1.5 test the values are little higher during the first meshes but get the expected values during the last meshes. The rates $r_{\parallel,\parallel_h}$ of the global error $\|u - u_h\|_h$ are higher than the expected values on the first meshes. This happens for all the *p*-test cases. Moving to the last refinement steps the $r_{\|.\|_h}$ tend to get the expected values for all *p*-cases. Here, we further add that the results in Table 2 are in agreement with the computations in [25] for the elliptic case, see also discussion in [34].

$u \in W^{2,p}(Q), \bar{Q} = [0:0.4] \times [0:0.4]$ with										
$u = ((x - 0.2)^2 + (t - 0.2)^2)^{\gamma}, \ \gamma = 2.1 - \frac{2}{p}, \ \varepsilon = 1,$										
errors	$\ \partial_t$	$u - \partial_t u_h \ $	L^2	$\ \mathbf{F}(\partial_t u)\ $	$u) - \mathbf{F}(\partial_t u)$	$u_h)\ _{L^2}$		$\ u-u_h\ _h$		
$\mathbf{p}:=$	p=1.15	p=1.25	p=1.5	p=1.15	p=1.25	p = 1.5	p=1.15	p=1.25	p=1.5	
Expected	0.12	0.95	0.22	0.12	0.95	0.22	0.0	0.2	0.5	
rates	0.13	0.25	0.33	0.13	0.25	0.33	0.2	0.3	0.5	
$h_0 = 0.2$				Cor	nputed ra	tes				
$h_s = \frac{h_0}{2^s}$	$r_t^{L^2}$	$r_t^{L^2}$	$r_t^{L^2}$	$r_{F,t}$	$r_{F,t}$	$r_{F,t}$	$r_{\parallel .\parallel_h}$	$r_{\parallel .\parallel_h}$	$r_{\parallel.\parallel_h}$	
s = 0	-	-	-	-	-	-	-	-	-	
s = 1	0.5827	0.3539	0.8626	0.5919	0.3632	0.8630	0.7747	0.6267	0.8656	
s=2	0.4137	0.2643	0.8346	0.4350	0.2932	0.8429	0.6675	0.6277	0.8149	
s = 3	0.2931	0.2795	0.7650	0.3127	0.2623	0.7848	0.4952	0.5040	0.8490	
s = 4	0.2363	0.2872	0.6660	0.2489	0.2710	0.6960	0.3522	0.4094	0.7290	
s = 5	0.2156	0.2928	0.5626	0.2249	0.2830	0.5949	0.2791	0.3592	0.6238	
s = 6	0.2094	0.2942	0.4785	0.2189	0.2911	0.5058	0.2529	0.3363	0.5254	
s = 7	0.2074	0.2967	0.4310	0.2183	0.3014	0.4406	0.2464	0.3248	0.5140	

Table 2: Example 2: point singularity case. Convergence rates $r_t^{L^2}$ and $r_{F,t}$ and $r_{\parallel \cdot \parallel_h}$

Line singularity test case In this test problem the domain is $\bar{Q} = [0.1:0.5] \times$ [0:0.4] and the exact solution is $u(x,t) = |x|^{\gamma_1}|t - 0.2|^{\gamma_2}$, with $\gamma_1 = 2 + \frac{1}{p}$ and $\gamma_2 = 2.11 - \frac{1}{p}$. The problem is solved for $p \in \{1.15, 1.25, 1.5\}$. We can verify that the solution u belongs to $W^{2,p}(Q)$, but we can see that it exhibits anisotropic regularity properties in x and t directions, with a singular behavior travelling across the points $\{(x, t), 0.1 \le x \le 0.5, t = 0.2\}$. Our goal is to investigate the convergence behavior of the three errors, i.e., the behavior of the rates, and how they are affected by the anisotropic regularity properties of u. Due to the reduced smoothness in the t-direction, it is expected that the converge properties of $||u-u_h||_h$ will be determined by the convergence of $\tau^{\lambda} \|\partial_t u - \partial_t u_h\|_{L^2}$, compare with the previous example. Table 3 shows the results of the numerical convergence rates. For each p-case, we can observe that the values of $r_t^{L^2}$ and $r_{F,t}$ are little higher than the theoretical predicted values, (i.e., the values in the line "expected rates") during the first meshes. However moving to the last mesh refinement steps the rates reduce and get the expected values derived by the error analysis. Also we observe that for all p-cases the values of $r_t^{L^2}$ and $r_{F,t}$ are in very good agreement, compare with Corollary 3.16 and Proposition 5.2. In the last columns in Table 3 the behavior of $r_{\|.\|_{h}}$ is given. For all meshes we can see that the values are higher than the corresponding values of $r_t^{L^2}$, as it was expected. Moving to the last meshes the values are getting lower and are approaching the expected values. However, we need to emphasize that for the test case p = 1.5 the rates of all errors appear to be higher than the expected value.

$u \in W^{2,p}(Q), \ Q = [0.1:0.5] \times [0:0.4] \text{ with} \\ u = x ^{\gamma_1} \ t ^{\gamma_2}, \ \gamma_1 = 2 + \frac{1}{p}, \ \gamma_2 = 2.11 - \frac{1}{p}, \ \varepsilon = 1,$										
errors	$\ \partial_t$	$u - \partial_t u_h \ $	L^2	$\ \mathbf{F}(\partial_t u)\ $	$\ \mathbf{F}(\partial_t u) - \mathbf{F}(\partial_t u_h)\ _{L^2}$			$\ u-u_h\ _h$		
p:=	p=1.15	p=1.25	p=1.5	p=1.15	p=1.25	p = 1.5	p=1.15	p=1.25	p=1.5	
Expected rates	0.17	0.25	0.38	0.17	0.25	0.38	0.27	0.38	0.58	
$h_0 = 0.2$		Computed rates								
$h_s = \frac{h_0}{2^s}$	$r_t^{L^2}$	$r_t^{L^2}$	$r_t^{L^2}$	$r_{F,t}$	$r_{F,t}$	$r_{F,t}$	$r_{F,x}$	$r_{F,x}$	$r_{F,x}$	
s = 0	-	-	-	-	-	-	-	-	-	
s = 1	0.5248	0.7147	0.8310	0.5248	0.7147	0.8310	0.7733	0.8661	0.9084	
s=2	0.3495	0.6722	0.8464	0.3495	0.6722	0.8464	0.5742	0.8111	0.9105	
s = 3	0.2187	0.5782	0.8569	0.2187	0.5782	0.8569	0.3605	0.7067	0.9101	
s = 4	0.1951	0.4671	0.8581	0.1951	0.4671	0.8581	0.2582	0.5682	0.9046	
s = 5	0.2043	0.3962	0.8433	0.2043	0.3962	0.8433	0.2303	0.4573	0.8877	
s = 6	0.2069	0.3589	0.8016	0.2069	0.3589	0.8016	0.2198	0.3908	0.8485	
s = 7	0.2048	0.3338	0.7273	0.2048	0.3338	0.7273	0.2134	0.3857	0.7775	

Table 3: Example 3: line singularity test. The values of the convergence rates $r_t^{L^2}$, $r_{F,t}$ and $r_{\|.\|_h}$.

4.2 Examples in three-dimensional space-time cylinders

Point Singularity in d = 3. The purpose of this example is to investigate the convergence behavior of the discretization error in time and in space separately, as well the behavior of the global error for the case of having three-dimensional spacetime cylinder. We compare the numerical results with the theoretical findings given in Lemma 3.15 and Theorem 3.19. Thus we consider the problem on $\bar{Q} = [0:0.4]^3$ with solution the radially symmetric function $u(x, y, t) = ((x - 0.2)^2 + (y - 0.2)^2 + (t - 0.2)^2)^{\frac{\gamma}{2}}$, with $\gamma = 2.25 - \frac{d}{p}$. Note that the singular point is located at the center of Q and $u \in W^{2,p}(Q)$. We solve the problem on several mesh refinement steps for $p \in \{1.6, 1.7, 1.85\}$ and $\varepsilon = 1$, and we compute the corresponding convergence rates of the errors $\|\mathbf{F}(\partial_t u) - \mathbf{F}(\partial_t u_h)\|_{L^2}$, $\|\mathbf{F}(\nabla_x u) - \mathbf{F}(\nabla_x u_h)\|_{L^2}$ and $\|u - u_h\|_h$. The numerical results are reported in Table 4. We can see that for all the mesh levels the convergence rates $r_{F,t}$ have good behavior and are nearly to the order of the expected rates. Similarly, in Table 4 we can see the good behavior of $r_{F,x}$ and $r_{\parallel,\parallel_h}$. In general their values are very close and are in agreement with the theoretical estimates. For the p = 1.85 test, we can observe that on the first coarse meshes the rates $r_{F,x}$ and $r_{\|.\|_h}$ appear to be little high. Note that for this test case the solution u has a slightly greater regularity, i.e., $u \in W^{2,2}$, than the theoretical limiting value, and this likely explains these high values. Anyway moving to more refined meshes the rates get progressively the expected values.

$u \in W^{2,p}(Q), Q = [0:0.4]^{d=3} u = \mathbf{x} - 0.2 ^{\gamma}$, with $\gamma = 2.25 - \frac{d}{p}, \varepsilon = 1$.									
errors	$\ \mathbf{F}(\partial_t$	$u) - \mathbf{F}(\partial_t u)$	$ u_h) _{L^2}$	$\ \mathbf{F}(abla_x)\ $	$(u) - \mathbf{F}(\nabla$	$(u_x u_h) \ _{L^2}$	$\ u-u_h\ _h$		
p:=	p=1.6	p=1.7	p=1.85	p=1.6	p=1.7	p=1.85	p=1.6	p=1.7	p=1.85
Expected rates	0.312	0.367	0.44	0.46	0.55	0.66	0.46	0.55	0.66
$h_0 = 0.2$				Con	nputed ra	ates			
$h_s = \frac{h_0}{2^s}$	$r_{F,t}$	$r_{F,t}$	$r_{F,t}$	$r_{F,x}$	$r_{F,x}$	$r_{F,x}$	$r_{\parallel .\parallel_h}$	$r_{\parallel .\parallel_h}$	$r_{\parallel .\parallel_h}$
s = 0	-	-	-	-	-		-	-	-
s = 1	0.3184	0.44962	0.2975	0.1535	0.3349	0.6331	0.5459	0.3299	0.6296
s=2	0.2892	0.4292	0.1513	0.4721	0.6047	0.9306	0.4764	0.6051	0.9061
s = 3	0.2924	0.3635	0.1102	0.4788	0.5394	0.8576	0.4816	0.5396	0.8244
s = 4	0.2994	0.3584	0.1954	0.4488	0.4842	0.8019	0.4519	0.4863	0.7715
s = 5	0.3071	0.3640	0.2632	0.4290	0.4527	0.7609	0.4324	0.4560	0.7360
s = 6	0.3117	0.3310	0.3133	0.4196	0.4350	0.7313	0.4232	0.4391	0.7121
s = 7	0.3150	0.3310	0.3592	0.4258	0.4466	0.7119	0.4294	0.4412	0.6972

Table 4: Example 4: $Q \subset \mathbb{R}^{d=3}$, point singularity: The values of the convergence rates $r_{F,t}$, $r_{F,x}$ and $r_{\parallel,\parallel_h}$.

Smooth solution, anisotropic meshes in d = 3. In the previous examples we have seen that the convergence rates $r_{F,t}$ have lower values than the corresponding $r_{F,x}$ rates. The purpose of this numerical test is to apply an anisotropic mesh refinement procedure for obtaining optimal convergence rates. This means that we will use an appropriate smaller mesh size in the direction of t, say h_t , compared to the mesh

size h_x in the x-direction, in order to recover optimal values for both $r_{F,t}$ and $r_{F,x}$. We consider the problem on $\bar{Q} = [0 : 0.4]^3$ with solution $u(x, y, t) = (x^2 + y^2 + y^2)^2$ $t^2)^{\frac{\gamma}{2}}$, with $\gamma = 5 + \frac{d}{p}$. Note that $u \in W^{2,2}(Q)$. We solve the problem for $p \in U^{2,2}(Q)$. $\{1.6, 1.7, 1.85\}$ and $\varepsilon = 0.01$. For this test case we set $\tau = 0.2h_t^{\lambda}$. First we solve the problem employing isotropic uniform mesh levels, i.e., $h_t \approx h_x$, and we compute the corresponding convergence rates of the errors $\|\mathbf{F}(\partial_t u) - \mathbf{F}(\partial_t u_h)\|_{L^2}$ and $\|\mathbf{F}(\nabla_x u) - \mathbf{F}(\partial_t u_h)\|_{L^2}$ $\mathbf{F}(\nabla_x u_h)\|_{L^2}$. The numerical results are reported in the first six columns in Table 5. For each of the three p-cases, we see that the convergence rates $r_{F,t}$ are close to the expected value 0.5. In the next three columns the rates $r_{F,x}$ are shown for the associated *p*-test cases. The rates are optimal with respect to the regularity of the solution and follow the theoretical convergence rates, compare with 'Smooth test case' above. For every p-case we solve again the problem using an anisotropic mesh refinement strategy where $h_t \approx h_x^{1.5}$. The last three columns in Table 5 contain the rates $r_{F,t}$ computed for this anisotropic mesh case. Here we observe that in all mesh levels the rates are improved and are close to the values of $r_{F,x}$ (before anisotropic meshing), which are optimal with respect to the solution regularity.

After applying the anisotropic mesh procedure described above with $h_t \approx h_x^{1.5}$, the approximation error $\tau^{-\lambda} \|\partial_t u - \partial_t v_h\|_{L^2(Q)}^2$ should have similar behavior with $\|\mathbf{F}(\nabla_x u) - \mathbf{F}(\nabla_x v_h)\|_{L^2}^2$. As a consequence the errors $\|\mathbf{F}(\nabla_x u) - \mathbf{F}(\nabla_x u_h)\|_{L^2}$ and $\|u - u_h\|_h$ must convergence with order close to one, because the solution is smooth and k = 1, see (3.42). The resulting values of $r_{F,x}$ and $r_{\|.\|_h}$ are summarized in Table 6. It can be seen that the rates have values close to the optimal order one for all p-test cases, as it was expected.

Remark 4.1. Consider for the moment the elliptic operator $-\operatorname{div} \mathbf{A}(\nabla_x u)$ of (3.1). The condition number of the associated Picard iterative matrix behaves as $c_p \varepsilon^{p-2} h^{-2}$, and for $1 , it increases while diminishing <math>\varepsilon$. It is known that this creates some numerical difficulties and more advanced techniques must be introduced, see discussion in [34]. However, without going into detail, from inequalities (3.13) and (3.8d) we can have

$$\int_{Q} c_{p,\varepsilon,\|v_{1,h}\|_{L^{\infty}},\|v_{2,h}\|_{L^{\infty}}} |\nabla(v_{1,h} - v_{2,h})|^{2} dx dt
\leq \int_{Q} \left(\mathbf{A}(\nabla_{x}v_{1,h}) - \mathbf{A}(\nabla_{x}v_{2,h}) \right) \cdot (v_{1,h} - v_{2,h}) \leq \int_{Q} c_{p,\varepsilon}^{m} |\nabla(v_{1,h} - v_{2,h})|^{2} dx dt,$$
(4.1)

for $v_{1,h}$, $v_{2,h} \in V_h^k$. Inequalities (4.1) can provide bounds for the eigenvalues of the Picard iterative matrix and thus an estimation of the condition number, [14]. For the particular values of the parameters that we use in the numerical test above, the condition number is not high. Thus the Picard iterative procedure performed well giving the expectable results in (maximum) seven iterations.

Conclusions

Space-time FE methods have been developed and analysed for solving quasilinear parabolic problems in space and in time in a unified way. The models are general-

$u \in W^{2,p}(Q), Q = [0:0.4]^{d=3} u = \mathbf{x} ^{\gamma}, \text{ with } \gamma = 5 + \frac{d}{p}, \varepsilon = 0.01.$									
errors	$\ \mathbf{F}(\partial_t u)\ $	$(\iota) - \mathbf{F}(\partial_t)$	$u_h)\ _{L^2}$	$\ \mathbf{F}(abla_x)\ $	$(u) - \mathbf{F}(\nabla$	$\ u_x u_h\ _{L^2}$	$\ \mathbf{F}(\partial_t u) - \mathbf{F}(\partial_t u_h)\ _{L^2}$		
p :=	p=1.6	p = 1.7	p=1.85	p=1.6	p=1.7	p=1.85	p=1.6	p=1.7	p=1.85
Expected rates	0.5	0.5	0.5	0.75	0.75	0.75	0.75	0.75	0.75
$h_0 = 0.2$		Computed rates anisotropic meshes							leshes
$h_s = \frac{h_0}{2^s}$	$r_{F,t}$	$r_{F,t}$	$r_{F,t}$	$r_{F,x}$	$r_{F,x}$	$r_{F,x}$	$r_{F,t}$	$r_{F,t}$	$r_{F,t}$
s = 0	-	-	-	-	-		-	-	-
s = 1	0.6581	0.6390	0.6042	0.8061	0.8156	0.9145	0.9025	0.6439	0.9389
s = 2	0.7315	0.6986	0.6526	0.7814	0.8268	0.8760	0.7995	0.7156	0.6099
s = 3	0.6653	0.6429	0.6272	0.7724	0.8076	0.8365	0.8082	0.7134	0.6914
s = 4	0.6263	0.6229	0.6313	0.7686	0.8078	0.7866	0.8192	0.7236	0.7185
s = 5	0.6152	0.6135	0.6048	0.7685	0.8091	0.7990	0.7864	0.7256	0.7298
s = 6	0.5743	0.5455	0.4984	0.7688	0.8062	0.7781	0.7617	0.7216	0.7403
s = 7	0.5527	0.4915	0.5148	0.7673	0.8020	0.7579	0.7637	0.7279	0.7476

Table 5: Example 5: $Q \subset \mathbb{R}^{d=3}$, anisotropic meshes: The values of the convergence rates before and after the anisotropic mesh refinement procedure.

izations of the parabolic *p*-Laplacian problem. The whole approach follows a timeupwind streamline methodology for stabilizing the discretization in time. A complete discretization error analysis was developed in a suitable quasinorm. The proposed method applied to problems having regular and less regular solutions. The method worked well for both cases and the numerical convergence rates were in agreement with the theoretical rates. Moreover numerical examples were performed for the case where the solution exhibits a different regularity behavior with respect to the space and to time direction.

The present work can be extended to the case of using discontinuous Galerkin discretizations in time. These type of schemes can be further combined with time-Domain Decomposition iterative solvers (DD) materialized in a parallel environment. This certainly will help in the direction of constructing efficient space-time methods for more general models, e.g., non-Newtonian fluid models, which are used for describing real world problems. The development of this type of numerical methods is the subject of a work in progress.

Acknowledgements

This work has been supported by the JKU-LIT project LIT-2017-4-SEE-004. The author would like to thank the Institute of Computational Mathematics of Johannes Kepler University Linz for hosting this project.

5 Appendix

Proof of Lemma 3.20:

$u \in W^{2,p}(Q), \ Q = [0:0.4]^{d=3} \ u = \mathbf{x} ^{\gamma}, \text{ with } \gamma = 5 + \frac{d}{p}, \ \varepsilon = 0.01.$								
errors	$\ \mathbf{F}(abla_x)\ $	$(u) - \mathbf{F}(\nabla$	$\ u_{x}u_{h}\ _{L^{2}}$		$ u-u_h $	h		
$\mathbf{p}:=$	p=1.6	p=1.7	p=1.85	p=1.6	p=1.7	p=1.85		
Expected rates	0.5	0.5	0.5	0.75	0.75	0.75		
$h_0 = 0.2$	Co	mputed r	anis	otropic n	neshes			
$h_s = \frac{h_0}{2^s}$	$r_{F,x}$	$r_{F,x}$	$r_{F,x}$	$r_{\parallel .\parallel h}$	$r_{\parallel .\parallel h}$	$r_{\parallel .\parallel h}$		
s = 0	-	-	-	-	-	-		
s = 1	1.2497	0.9048	0.904	1.2309	0.8622	0.9145		
s=2	1.4039	1.2314	1.2862	1.3846	1.2124	1.2062		
s = 3	1.4161	1.2446	1.2427	1.3937	1.2221	1.1923		
s = 4	1.4163	1.2553	1.2359	1.3934	1.2317	1.1941		
s = 5	1.2386	1.1371	1.1619	1.2301	1.1314	1.1513		
s = 6	1.1294	1.0621	1.1811	1.1300	1.0673	1.1658		
s = 7	1.1173	1.1366	1.1734	1.1109	1.1315	1.1630		

Table 6: Example 5: $Q \subset \mathbb{R}^{d=3}$, anisotropic meshes: The optimal behavior of $r_{F,x}$ and $r_{\parallel,\parallel,h}$ with respect to the order k = 1 of the polynomial space

Proof. The second derivative of φ has the form, see Remark 3.1,

$$\varphi''(x) = \frac{\varepsilon + (p-1)x}{(\varepsilon + x)^{3-p}},\tag{5.1}$$

and for all $\varepsilon > 0, x \ge 0$ it holds

$$c_6(\varepsilon+x)^{p-2} \le \varphi''(x) \le p(\varepsilon+x)^{p-2},\tag{5.2}$$

where $c_6 := \min(1, p - 1)$. Utilizing (5.1) in (3.8a) and (3.8d), we have

$$\left(\int_{Q} |\nabla_{x}u - \nabla_{x}\Pi_{h}u|^{p} dx dt\right)^{\frac{1}{p}}$$

$$= \left(\int_{Q} |\nabla_{x}u - \nabla_{x}\Pi_{h}u|^{p} \varphi'' (|\nabla_{x}u| + |\nabla_{x}\Pi_{h}u|)^{\frac{p}{2}} \frac{1}{\varphi'' (|\nabla_{x}u| + |\nabla_{x}\Pi_{h}u|)^{\frac{p}{2}}} dx dt\right)^{\frac{1}{p}}$$

$$\leq C \left(\int_{Q} |\mathbf{F}(\nabla_{x}u) - \mathbf{F}(\nabla_{x}\Pi_{h}u)|^{p} \frac{1}{(\varepsilon + |\nabla_{x}u| + |\nabla_{x}\Pi_{h}u|)^{\frac{p(p-2)}{2}}} dx dt\right)^{\frac{1}{p}}$$
(5.3)

By applying Hölder's inequality (2.5a) in $L^{\frac{2}{p}}(Q)$ and $L^{\left(\frac{2}{p}\right)'}(Q) = L^{\frac{2}{2-p}}(Q)$ we obtain

$$\left(\int_{Q} |\nabla_{x}u - \nabla_{x}\Pi_{h}u|^{p} dx dt\right)^{\frac{1}{p}} \leq C \left(\int_{Q} |\mathbf{F}(\nabla_{x}u) - \mathbf{F}(\nabla_{x}\Pi_{h}u)|^{2} dx dt\right)^{\frac{1}{2}} \left(\int_{Q} (\varepsilon + |\nabla_{x}u| + |\nabla_{x}\Pi_{h}u|)^{p} dx dt\right)^{\frac{(2-p)}{2p}},$$
(5.4)

where the last term on the right hand side is finite due to the regularity assumptions.

Remark 5.1. Let us consider the case $p \ge 2$. We have that $\varphi''(x) \ge c_6(\varepsilon + x)^{p-2}$. Therefore, utilizing (3.8a) and (3.8d) we obtain

$$\|u - u_h\|_{L^p(Q)}^p \lesssim \int_Q |\nabla_x u - \nabla_x u_h|^p \, dx dt$$

$$= \int_Q |\nabla_x u - \nabla_x u_h|^2 \varphi'' \left(|\nabla_x u| + |\nabla_x u_h|\right) \frac{|\nabla_x u - \nabla_x u_h|^{p-2}}{\varphi'' \left(|\nabla_x u| + |\nabla_x u_h|\right)} dx dt$$

$$\lesssim \int_Q |\mathbf{F}(\nabla_x u) - \mathbf{F}(\nabla_x u_h)|^2 \frac{\left(|\nabla_x u| + |\nabla_x u_h|\right)^{p-2}}{c_6 \left(\varepsilon + |\nabla_x u| + |\nabla_x u_h|\right)^{p-2}} dx dt$$

$$\lesssim \int_Q |\mathbf{F}(\nabla_x u) - \mathbf{F}(\nabla_x u_h)|^2 \, dx dt.$$
(5.5)

Proceeding as in Lemma 3.15 and using (5.5) into (3.42) we can obtain

$$c_{\delta,m}\Big(\|u-u_{h}\|_{L^{2}(\Sigma_{T})}^{2}+\sum_{E\in\mathcal{T}_{h}}\tau^{\lambda}\|\partial_{t}u-\partial_{t}u_{h}\|_{L^{2}(E)}^{2}+\int_{Q}|\nabla_{x}u-\nabla_{x}u_{h}|^{p}\,dxdt\Big)$$

$$\leq C_{\delta,M}\Big(\tau^{-\lambda}\|\partial_{t}u-\partial_{t}v_{h}\|_{L^{2}(Q)}^{2}+\|u-v_{h}\|_{L^{2}(\Sigma_{T})}^{2}$$

$$+\sum_{E\in\mathcal{T}_{h}}\tau^{\lambda}\|\partial_{t}u-\partial_{t}v_{h}\|_{L^{2}(E)}^{2}+\int_{Q}|\mathbf{F}(\nabla_{x}u)-\mathbf{F}(\nabla_{x}v_{h})|^{2}\,dxdt\Big).$$
(5.6)

Proposition 5.2. Let the solution u as in Lemma 3.15, and let the interpolant $\Pi_h u$ as in Lemma 3.17. Then we have the following interpolation estimates

$$\sum_{E \in \mathcal{T}_h} \int_E |\partial_t u - \partial_t \Pi_h u|^2 \, dx \, dt \gtrsim \sum_{E \in \mathcal{T}_h} \int_E |\mathbf{F}(\partial_t u) - \mathbf{F}(\partial_t \Pi_h u)|^2 \, dx \, dt, \tag{5.7a}$$

$$\left(\int_{Q} |\partial_{t}u - \partial_{t}\Pi_{h}u|^{p} dx dt\right)^{\frac{1}{p}} \lesssim c_{*} \left(\int_{Q} |\mathbf{F}(\partial_{t}u) - \mathbf{F}(\partial_{t}\Pi_{h}u)|^{2} dx dt\right)^{\frac{1}{2}}, \qquad (5.7b)$$

where the constant c_* has similar form as in (3.52).

Proof. We recall that $c_6(\varepsilon + x)^{p-2} \leq \varphi''(x) \leq p(\varepsilon + x)^{p-2}$, see (5.1) and (5.2). Consequently, applying (3.13a) for real numbers a, b, we have $|a-b|^2\varphi''(0) \gtrsim |a-b|^2\varphi''(|a|+|b|)$. Replacing a, b with $\partial_t u$ and $\partial_t \Pi_h u$ and then using the relations given in Lemma (3.2), we find

$$\int_{E} |\partial_{t}u - \partial_{t}\Pi_{h}u|^{2} dx dt \gtrsim \int_{E} |\partial_{t}u - \partial_{t}\Pi_{h}u|^{2} \varphi''(|\partial_{t}u| + |\partial_{t}\Pi_{h}u|) dx dt$$

$$\gtrsim \int_{E} |\mathbf{F}(\partial_{t}u) - \mathbf{F}(\partial_{t}\Pi_{h}u)|^{2} dx dt,$$
(5.8)

and summing over all $E \in \mathcal{T}_h$ we get (5.7a).

To prove (5.7b), we use the relations given in Lemma (3.2) and (2.5a)

$$\begin{split} \int_{Q} \left|\partial_{t}u - \partial_{t}\Pi_{h}u\right|^{p} dx dt &= \int_{Q} \left(\left|\partial_{t}u - \partial_{t}\Pi_{h}u\right|^{2}\varphi''\left(\left|\partial_{t}u\right| + \left|\partial_{t}\Pi_{h}u\right|\right)\right)^{\frac{p}{2}} \frac{1}{\varphi''\left(\left|\partial_{t}u\right| + \left|\partial_{t}\Pi_{h}u\right|\right)^{\frac{p}{2}}} dx dt \\ &\lesssim \int_{Q} \left|\mathbf{F}(\partial_{t}u) - \mathbf{F}(\partial_{t}\Pi_{h}u)\right|^{p} \frac{1}{\left(\varepsilon + \left|\partial_{t}u\right| + \left|\partial_{t}\Pi_{h}u\right|\right)^{\frac{p(p-2)}{2}}} dx dt \\ &\lesssim \left(\int_{Q} \left|\mathbf{F}(\partial_{t}u) - \mathbf{F}(\partial_{t}\Pi_{h}u)\right|^{2}\right)^{\frac{p}{2}} \left(\int_{Q} \left(\varepsilon + \left|\partial_{t}u\right| + \left|\partial_{t}\Pi_{h}u\right|\right)^{p} dx\right)^{\frac{(2-p)}{2}}. \end{split}$$
(5.9)

Taking the $\frac{1}{p} - th$ power in (5.9) and setting $c_* := \left(\int_Q (\varepsilon + |\partial_t u| + |\partial_t \Pi_h u|)^p dx \right)^{2p}$ we get (5.7b).

References

- R. A. Adams and J. J. F. Fournier. Sobolev Spaces, volume 140 of Pure and Applied Mathematics. ACADEMIC PRESS-imprint Elsevier Science, second edition, 2003.
- [2] R. Adreev. Stability of sparse space-time finite element discretizations of linear parabolic evolution equations. IMA J. Numer. Anal., 33(1):242–260, 2013.
- [3] I. Babuška and T. Janik. The h-p version of the finite element method for parabolic equations. Part I. the p-version in time. Numerical Methods for Partial Differential Equations, 5(4):363–399, 1989.
- [4] I. Babuška and T. Janik. The h-p version of the finite element method for parabolic equations. II. the h-p version in time. Numerical Methods for Partial Differential Equations, 6(4):343–369, 1990.
- [5] J. W. Barrett and W. B. Liu. Finite element approximation of the parabolic p-Laplacian. SIAM J. Numer. Anal, 31(2):413–428, 1994.
- [6] D. Braess. *Finite elements.* Cambridge University Press, Cambridge, third edition, 2007. Theory, fast solvers, and applications in elasticity theory, Translated from the German by Larry L. Schumaker.
- [7] S. Brenner and L. Scott. *The Mathematical Theory of Finite Element Methods*. Texts in applied mathematics. Springer, New-York, 2nd Edition edition, 2008.
- [8] N. Chegini and R. Stevenson. Adaptive wavelet schemes for parabolic problems: Sparse matrices and numerical results. SIAM. J. Numerical Analysis, 49(1):182– 212, 2011.
- [9] E. DiBenedetto. Degenerate Parabolic Equations. Universitext. Springer, N.Y., New York, 1993.

- [10] L. Diening, C. Ebmeyer, and M. Růžička. Optimal convergence for the implicit space-time discretization of parabolic systems with *p*-structure. *SIAM J. Numer. Anal.*, 45(2):457–472, 2007.
- [11] L. Diening and M. Růžička. Interpolation operators in Orlicz-Sobolev spaces. Numer. Math., 107(1):107–129, 2007.
- [12] K. Eriksson and C. Johnson. Error estimates and automatic time step control for nonlinear parabolic problems I. SIAM Journal on Numerical Analysis, 24:12–23, 1987.
- [13] L. C. Evans. Partial Differential Equestions, volume 19 of Graduate Studies in Mathematics, USA. American Mathematical Society, 2nd Edition edition, 2010.
- [14] I. Faragó and J. Karatson. Numerical Solution of Nonlinear Elliptic Problems Via Preconditioning operators: Theory and Applications, volume 11. Nova Science Publishers, Inc, New York, 2002.
- [15] L. P. Franca, G. Hauke, and A. Masud. Revisiting stabilized finite element methods for the advective-diffusive equation. *Computer Methods in Applied Mechanics and Engineering*, 195:1560–1572, 2006.
- [16] P. Hansbo. Space-time oriented streamline diffusion methods for non-linear conservation laws in one dimension. Communications in Numerical Methods in Engineering, 10(3):203–215, 1994.
- [17] C. Hofer, U. Langer, M. Neumüller, and I. Toulopoulos. Time-multipatch discontinuous Galerkin space-time isogeometric analysis of parabolic evolution problems. *Electronic Transactions on Numerical Analysis.*, 49:126–150, 2018.
- [18] T. J.R. Hughes and G. M. Hulbert. Space-time finite element methods for elastodynamics:formulations and error estimates. *Comput. Methods Appl. Mech. Engrg.*, 66:339–363, 1988.
- [19] D. Kröner, M. Růžička, and I. Toulopoulos. Numerical solutions of systems with (p, δ)-structure using local discontinuous Galerkin finite element methods. Int. J. Numer. Methods Fluids, 76:855–874, 2014.
- [20] U. Langer and O. Steinbach. Space-Time Methods: Applications to Partial Differential Equations, volume 25 of Radon Series on Computational and Applied Mathematics. Walter de Gruyter GmbH and Co KG, 2019.
- [21] U. Langer and I. Toulopoulos. Analysis of multipatch discontinuous Galerkin IgA approximations to elliptic boundary value problems. *Computing and Visualization in Science*, 17:217–233, 2016.
- [22] S. Larsson and M. Molteni. Numerical solution of parabolic problems based on a weak space-time formulation. *Computational Methods in Applied Mathematics*, 17(1):65–84, 2016.

- [23] A. Mantzaflaris, F. Scholz, and I. Toulopoulos. Low-rank space-time decoupled isogeometric analysis for parabolic problems with varying coefficients. *Comput. Mathods Appl. Math*, 19(1):123–136, 2019.
- [24] C. Mollet. Stability of Petrov-Galerkin discretizations: Application to the spacetime weak formulation for parabolic evolution problems. *Computational Methods* in Applied Mathematics, 14(2):231–255, 2014.
- [25] S. Nakov and I. Toulopoulos. Convergence estimates of finite elements for a class of quasilinear elliptic problems. *uner review*, Preprint available as JKU-NUMA report:https://www.numa.uni-linz.ac.at/Publications/N/2020/, 2020.
- [26] T. Roubíček. Nonlinear Partial Differential Equations with Applications, volume 153 of ISNM, International Series of Numerical Mathematics. Birkhäuser Verlag, 2005.
- [27] A. Schafelner. Space-time finite element methods for parabolic initial-boundary problems. Master's thesis, Institute of Computational Mathematics, Johannes Kepler University Linz, 2017.
- [28] C. Schwab and R. Stevenson. Space-time adaptive wavelet methods for parabolic evolution problems. *Math. Comp.*, 78:1293–1318, 2009.
- [29] O. Steinbach. Space-time finite element methods for parabolic problems. Comp. Methods Appl. Math., 15(4):551–556, 2015.
- [30] T. E. Tezduyar. Stabilized finite element formulations for incompressible flow computations. Advances in Applied Mechanics, 28:1–44, 1992.
- [31] T. E. Tezduyar and K. Takizawa. Space time computations in practical engineering applications: a summary of the 25 - year history. *Comput Mech*, 63:747 - 753, 2019.
- [32] V. Thomée. Galerkin Finite Element Methods for Parabolic Problems, volume 25 of Springer Series in Computational Mathematics. Springer-Verlag Berlin Heidelberg, 2nd edition, 2006.
- [33] I. Toulopoulos. Space-time finite element methods stabilized using bubble function spaces. Applicable Analysis, 99(7):1153–1170, 2018.
- [34] I. Toulopoulos and T. Wick. Numerical methods for power-law diffusion problems. SIAM J. Sci. Comput., 39(3):A681–A710, 2017.
- [35] J. Cesenek and M. Feistauer. Theory of the space-time discontinuous galerkin method for nonstationary parabolic problems with nonlinear convection and diffusion. SIAM Journal on Numerical Analysis, 50(3):1181–1206, 2012.
- [36] Z. Yanyan and C. Zuchi. The first boundary value problem for strongly degenerate quasilinear parabolic equations in anisotropic Sobolev spaces. Acta Mathematica Scientia, 26(2):255 – 264, 2006.
- [37] E. Zeidler. Nonlinear Functional Analysis and its Applications: II/B: Nonlinear Monotone Operators. Springer-Verlag, New York, 1990.

Latest Reports in this series

2009 - 2018

[..]

2019

2019-01	Helmut Gfrerer and Jiří V. Outrata	
	On a Semismooth [*] Newton Method for Solving Generalized Equations	April 2019
2019-02	Matúš Benko, Michal Červinka and Tim Hoheisel	
	New Verifiable Sufficient Conditions for Metric Subregularity of Constraint Sys-	June 2019
	tems with Applications to Disjunctive Programs	
2019-03	Matúš Benko	
	On Inner Calmness [*] , Generalized Calculus, and Derivatives of the Normal- cone Map	October 2019
2019-04	Rainer Schneckenleitner and Stefan Takacs	
	Condition number bounds for IETI-DP methods that are explicit in h and p	December 2019
2019-05	Clemens Hofreither, Ludwig Mitter and Hendrik Speleers	
	Local multigrid solvers for adaptive Isogeometric Analysis in hierarchical spline spaces	December 2019
2020		
2020-01	Ioannis Toulopoulos	
	Viscoplastic Models and Finite Element Schemes for the Hot Rolling Metal	February 2020
	Process	
2020-02	Rainer Schneckenleitner and Stefan Takacs	
	Convergence Theory for IETI-DP Solvers for Discontinuous Galerkin Isogeo-	May 2020
	metric Analysis That Is Explicit in h and p	
2020-03	Svetoslav Nakov and Ioannis Toulopoulos	
	Convergence Estimates of Finite Elements for a Class of Quasilinear Elliptic	May 2020
	Problems	
2020-04	Helmut Gfrerer, Jiří V. Outrata and Jan Valdman	
	On the Application of the Semismooth [*] Newton Method to Variational Inequal- ities of the Second Kind	July 2020

$\boldsymbol{2021}$

2020-01 Ioannis Toulopoulos *A Continuous Space-Time Finite Element Scheme for Quasilinear Parabolic* February 2021 *Problems*

From 1998 to 2008 reports were published by SFB013. Please see

http://www.sfb013.uni-linz.ac.at/index.php?id=reports From 2004 on reports were also published by RICAM. Please see

http://www.ricam.oeaw.ac.at/publications/

For a complete list of NuMa reports see

http://www.numa.uni-linz.ac.at/Publications/List/